https://doi.org/10.5194/egusphere-2026-875
Preprint. Discussion started: 24 February 2026

Characterizing the Global Tropospheric Budget of Oxidized Nitrogen (NO_y)

Ishir Dutta[1], Colette L. Heald[2], Ilann Bourgeois[3], John D. Crounse[4], Eric J. Hintsa[5,6], Fred L. Moore[5,6], Jeff Peischl[5,7,a]

[1]Department of Earth, Atmospheric and Planetary Sciences, Massachusetts Institute of Technology, Cambridge, MA, USA
[2]Institute for Atmospheric and Climate Science, ETH Zürich, Zürich, Switzerland
[3]Univ. Savoie Mont Blanc, INRAE, CARRTEL, Thonon-Les-Bains, France
[4]Division of Geological and Planetary Sciences, California Institute of Technology, Pasadena, CA, USA
[5]Cooperative Institute for Research in Environmental Sciences, University of Colorado Boulder, Boulder, CO, USA
[6]Global Monitoring Laboratory, National Oceanic and Atmospheric Administration, Boulder, CO, USA
[7]Chemical Sciences Laboratory, National Oceanic and Atmospheric Administration, Boulder, CO, USA
[a]now at: Global Monitoring Laboratory, National Oceanic and Atmospheric Administration, Boulder, CO, USA

Correspondence to: Ishir Dutta (ishir@alum.mit.edu), Colette L. Heald (colette.heald@env.ethz.ch)

Abstract. Nitrogen oxides (NO_x = NO + NO_2) in the troposphere form an array of secondary pollutants that are detrimental to air quality, ecosystems, and climate. The family of reactive oxidized nitrogen (NO_y) in the atmosphere consists of NO_x and its reservoir species (e.g. HNO_3, PAN). Our understanding of the processes underlying the transformation of NO_y has advanced considerably over recent decades, however, the relative importance of NO_y partitioning and loss pathways remain uncertain. In this study, we use the GEOS-Chem global chemical transport model and observations from the ATom flight campaign to assess the simulated global budget of tropospheric NO_y, and the production and loss fluxes between key NO_y species. Our simulation indicates that the mean global chemical lifetime of NO_x is ~21 hours and the mean global deposition lifetime of NO_y is 5.5 days. The global mean NO_x:NO_y ratio at the surface is 0.23 (over continents it is 0.34) and at 500 hPa is 0.10. In addition to the four most prevalent gas-phase species (NO, NO_2, HNO_3, PAN) that have been central to previous descriptions of tropospheric NO_y chemistry, we find that other species play key roles in driving overall chemical cycling. The model representation of organic nitrate chemistry is highly simplified and likely overestimates the importance of hydrolysis as a sink while underestimating deposition. Finally, the photolytic loss of particulate nitrate (pNO_3^-) to form NO_2 and HONO, as represented in our simulations, is comparable to its depositional loss, indicating the importance of further constraining this photolysis sink.

1 Introduction

Nitrogen oxides (NO_x = NO + NO_2) are a key driver of tropospheric chemistry and form a range of secondary pollutants, including ozone (O_3) and particulate matter (PM), that affect air quality, ecosystems, and climate. In the atmosphere, NO_x catalyzes the production of tropospheric ozone, which has negative impacts on human health and climate. Ozone is also a precursor to the hydroxyl (OH) radical, which is a crucial oxidant that determines the rate at which many reactive

https://doi.org/10.5194/egusphere-2026-875
Preprint. Discussion started: 24 February 2026

compounds are removed from the atmosphere. Direct removal of reactive nitrogen species by wet or dry deposition may also have profound effects on ecosystems. Excess nitrogen deposition causes acid rain and eutrophication, which may be responsible for the loss of biodiversity in pH- or nutrient-sensitive terrestrial and aquatic ecosystems (Likens and Bormann, 1974; Paerl and Whitall, 1999; Schindler, 1974).

Emitted NO_x can be transformed, through oxidative processes, into a broader class of oxidized nitrogen compounds (NO_y). These include short-lived species such as the nitrate radical (NO_3), nitrous acid (HONO), peroxynitric acid (HNO_4) and species with moderate to longer lifetimes such as nitric acid (HNO_3) and peroxyacyl nitrates (PANs) (Seinfeld and Pandis, 2016). The short-lived species drive chemical processing near source regions, while longer-lived species can function as reservoirs of NO_x, advecting NO_y away from source regions and releasing NO_x into remote environments.

NO_x is emitted into the atmosphere from a mixture of anthropogenic and natural sources (for recent global estimates see: Crippa et al., 2018; Hoesly et al., 2018; McDuffie et al., 2020). The dominant source of tropospheric NO_x is the burning of fossil fuels. High combustion temperatures convert atmospheric nitrogen (N_2) to nitric oxide (NO) via the Zel'dovich mechanism (thermal NO_x)(Lavoie et al., 1970; Zel'dovich, 1946) and oxidize nitrogen within the fuels (fuel NO_x)(Merryman and Levy, 1977). Natural sources of NO_y emissions include microbial activity in soil, biomass burning, lightning, and small quantities of alkyl nitrates from the ocean. NO_x is emitted primarily as NO, which is oxidized by O_3, the hydroperoxy radical (HO_2), or organic peroxy radicals (RO_2) to form nitrogen dioxide (NO_2). During the day, NO_2 is photolyzed back into NO, thereby forming the NO_x chemical family. Nitrous acid (HONO) and peroxynitric acid (HNO_4) also rapidly cycle with NO_x during the day – HONO is primarily formed by the oxidation of NO by OH and photolyzes back to NO, while HNO_4 is a weakly-bound molecule formed from the association reaction of NO_2 and HO_2 and decomposes back to precursors at warm temperatures. The main reservoir species for NO_x is peroxyacetyl nitrate (PAN), which is an example of a peroxyacyl nitrate, compounds that are formed when peroxyacyl radicals react with NO_2. These PANs are thermally unstable and dissociate to release NO_x into the remote atmosphere, making them a reservoir for NO_y. A key loss pathway for NO_x is the oxidation of NO_2 during the daytime by OH to form nitric acid (HNO_3). At night, when photolysis shuts down, NO_2 instead reacts with O_3 to form the nitrate radical (NO_3). NO_3 may react with more NO_2 to form dinitrogen pentoxide (N_2O_5), which can hydrolyze to form nitric acid (HNO_3). Another major loss pathway for NO_x is the formation of organic nitrates, either via the reaction of NO with peroxy radicals or by the oxidation of volatile organic compounds (VOCs) by NO_3. The fate of these gas-phase nitrates is uncertain, but generally they may be removed by deposition or undergo further photo-oxidation, which can either recycle NO_x or form larger, more functionalized nitrates that may partition into the aerosol phase. Several organic nitrates are thought to hydrolyze rapidly in the condensed phase to form HNO_3. Nitric acid is highly soluble and may be neutralized to form nitrate aerosol (pNO_3^-), often by ammonia (NH_3), the primary base in the troposphere. This total nitrate system ($TNO_3 = HNO_3 + pNO_3^-$) is generally considered to be the major terminal sink of NO_y. Therefore, the formation and subsequent removal (by wet or dry deposition) of TNO_3 from the atmosphere is key in determining the lifetime of NO_y. These species are the more prevalent forms of NO_y, though there are many additional, typically shorter-lived, compounds. See Seinfeld and Pandis (2016) for further details on the canonical chemistry described above.

https://doi.org/10.5194/egusphere-2026-875
Preprint. Discussion started: 24 February 2026

Given the central role of NO_x in tropospheric chemistry, NO_y species have been represented since the advent of tropospheric models (e.g. Crutzen and Zimmermann, 1991; Levy II, 1972, 1973; Logan et al., 1981), with a particular focus on the NO_y budget in Logan (1983). The importance of PAN as an organic reservoir for NO_x was highlighted by Singh and Hanst (1981). Subsequent modeling studies pointed to PAN as an important source of NO_x in the low-altitude remote troposphere (Kasibhatla et al., 1993; Moxim et al., 1996) and to uncertain PAN photochemistry and deposition which resulted in high-biased model representations of this species (Horowitz et al., 2003; Jacob et al., 1993). Other simultaneous studies of NO_y highlighted the challenge of modeling HNO_3 and indicated possible unknown HNO_3 loss processes (Wang et al., 1998b). Subsequent work established the importance of lightning to NO_x concentrations especially in the upper troposphere, as well as the relative importance of PAN and HNO_3 as reservoir species in the upper and lower troposphere respectively (Singh et al., 2007; Staudt et al., 2003).

More recent global modeling studies emphasize the same key species, but large differences in the representation of NO_y remain. Murray et al. (2021) show that the tropospheric burden of NO_y varies by almost a factor of 4 across the ACCMIP models, with similarly large differences in speciation. Many model schemes now treat evermore complex cycling of organic compounds in the troposphere, including the representation of organic nitrogen (e.g. Bates et al., 2022; Bates and Jacob, 2019; Bian et al., 2017; Fisher et al., 2016; Huijnen et al., 2010; Sander et al., 2019). However, there still exist many gaps in our understanding of the chemical cycling of NO_y and the loss pathways that may contribute to model spread.

Nitrous acid (HONO) is a major source of uncertainty in chemical transport models. It has long been known as an important source of OH radicals in the morning (Perner and Platt, 1979), with uncertainties in heterogeneous chemistry limiting our understanding of the impacts on NO_y and oxidant burdens (Akimoto et al., 1987; Jacob, 2000; Pitts Jr. et al., 1984). Recent work has sought to explain elevated observations of HONO made in the remote troposphere which could influence global oxidant chemistry (Kasibhatla et al., 2018; Rowlinson et al., 2025).

The status of aerosol nitrate as a permanent sink for NO_y has come into question in recent years, with a several studies noting the production of NO_2 and HONO by photolysis of pNO_3^- (renoxification) (Andersen et al., 2023; Reed et al., 2017; Ye et al., 2016a, b, 2017). This recycling would enable freshly-produced NO_x to drive the formation of secondary pollutants in pristine environments (Honrath et al., 1999). However, the rate of this photolysis is poorly constrained and has been shown to be dependent on the composition of the particles – initial studies suggested that the photolysis rate constant ranged from one to three orders of magnitude higher than that of HNO_3 and depended on the substrate on which particles were photolyzed (Baergen and Donaldson, 2013; Ye et al., 2016a). However, some recent lab and field studies have suggested a much more moderate photolysis rate constant between 1-30 times faster than that of HNO_3 (Romer et al., 2018; Shi et al., 2021). Recent modeling studies have set a rate for J_{NO3-} that is 100 times faster than J_{HNO3} (Kasibhatla et al., 2018; Shah et al., 2023).

Due to the importance of NO_x as a pollutant itself and as a precursor to tropospheric ozone, a greenhouse gas and also a key air pollutant, NO_x emissions have been subject to national emission control policies around the world. For example, in the United States, such emissions controls have been responsible for a 73% decrease in anthropogenic NO_x emissions between 1990 and 2023 (US EPA, 2024). Many studies have used satellite observations of NO_2 to constrain NO_x emissions and trends

https://doi.org/10.5194/egusphere-2026-875
Preprint. Discussion started: 24 February 2026

worldwide, particularly in response to such regulatory measures (Martin et al., 2003; Miyazaki et al., 2017). While such reductions are largely beneficial to air quality in the near-field, there can be consequences for NO_y cycling further away from sources. For example, it has been shown that reductions in anthropogenic emissions increase the importance of organic nitrate formation (Zare et al., 2018). Such changes can lead to greater export of NO_x from source regions to more remote ones, thereby making the formation of secondary pollutants derived from NO_y chemistry a regional-scale problem rather than a local one (Romer Present et al., 2020). Both the natural sources of NO_x and the formation and fate of organic nitrates are highly uncertain; however, they are essential when attempting to constrain NO_x lifetimes (Browne and Cohen, 2012).

In this work, we characterize the global tropospheric budget for NO_y as represented in a state-of-the-science global model. We go beyond previous work that has focused on a handful of key NO_y species, to provide a more comprehensive accounting of tropospheric NO_y. In addition to emissions, burdens, removal rates, and lifetimes of NO_y species, we also characterize the relative importance of the various processes and species that drive NO_y chemistry. The goal of this study is to assess rather than improve the global NO_y budget as currently simulated. The systematic framework developed here allows us to explore how uncertainties within a single process impact the NO_y system as a whole and thus provides future opportunities to improve our understanding of NO_y cycling.

2 Methods

2.1 Model Description

We use v14.3.0 of the GEOS-Chem global chemical transport model (www.geos-chem.org), driven by Modern-Era Retrospective analysis for Research and Applications, Version 2 (MERRA-2) assimilated meteorology. Simulations are spun up for 6 months and are conducted at a horizontal resolution of 2° x 2.5°, 47 vertical hybrid sigma-pressure levels, and a chemistry timestep of 20 minutes and transport timestep of 10 minutes (Philip et al., 2016).

The model includes a simulation of HO_x-NO_x-VOC-O_3-halogen chemistry (Bates and Jacob, 2019; Wang et al., 2021) coupled to aerosol thermodynamics (Park et al., 2004; Pye et al., 2009). Alkyl (methyl, ethyl, and propyl) nitrate chemistry (Fisher et al., 2018) and aromatic oxidation products (Bates et al., 2021) contribute to the organic nitrate burden. Aerosol nitrate (pNO_3^-) photolysis is based on Kasibhatla et al. (2018), with modifications made by Shah et al. (2023) to account for the internal mixing of fine mode pNO_3^- in sea salt aerosol. In this model representation, the photolysis of pNO_3^- forms HONO and NO_2 in a molar ratio of 2:1, with a rate set by scaling the photolysis rate constant of HNO_3 by an "enhancement factor" (EF) of 100. Partitioning of nitric acid between the gas phases and fine mode nitrate aerosol (NIT) is calculated using the ISORROPIA II model (Fountoukis and Nenes, 2007). Coarse mode nitrate aerosol (NITs) is formed by the neutralization of nitric acid by sea salt to form $NaNO_3$. A full list of nitrogen-containing species and their properties, as included in this version of GEOS-Chem, is given in Table S1 in the Supporting Information.

Anthropogenic emissions (including ship emissions) follow the year-specific global Community Emissions Data System inventory (CEDSv2) (Hoesly et al., 2018; McDuffie et al., 2020). Ship NO_x emissions are subject to a parameterization of

https://doi.org/10.5194/egusphere-2026-875
Preprint. Discussion started: 24 February 2026

NO_x chemistry within plumes (PARANOX)(Holmes et al., 2014) in order to better represent the production of HNO_3 and O_3, and therefore contribute to a "direct" source of HNO_3. We use the Global Fire Emissions Database (GFED4.1s) for biomass burning emissions. Dust (Fairlie et al., 2007; Ridley et al., 2012), biogenic VOCs (Guenther et al., 2012; Hu et al., 2015), sea salt, soil NO_x (Hudman et al., 2012) and lightning NO_x (Murray et al., 2012) are specified from offline year-specific archived emissions (Weng et al., 2020).

Wet deposition in GEOS-Chem includes two mechanisms – the scavenging of gases and aerosol by wet convective updrafts, and their removal by large-scale precipitation, as described by Liu et al., (2001) for water-soluble aerosols, and Amos et al., (2012) for gases. Removal by precipitation may occur in-cloud ("rainout") or below-cloud ("washout"). We do not use the optional modified wet deposition scheme from Luo et al. (2019, 2020). Dry deposition is represented by a resistances-in-series model (Wesely, 1989), implemented by Wang et al. (1998a), with size dependent aerosol dry deposition from Emerson et al. (2020) which is based on Zhang et al. (2001). Dry deposition depends on land cover type, local meteorology, and the reactivity, solubility, and hygroscopicity (which affects particle radius) of the compounds being deposited.

We perform a set of simulations from July 2016 to May 2018 and sample the model along the observed flight tracks (see Section 2.2). For the annual budget, we perform a year-long simulation for 2016, adding chemical production and loss tracer variables in the Kinetic PreProcessor (KPP v3.0.2)(Lin et al., 2023; Sandu et al., 2023) to every reaction relevant to NO_y chemistry in order to characterize the annual chemical flux between NO_y species in the model (see Table S2 in the Supporting Information). We add three new species to better account for reactive nitrogen mass in organic aerosol: ALKONITA (alkyl nitrate aerosol), IDNITA (aerosol formed by isoprene dinitrate uptake), $INDIOL_N$ (hydrolysis product of IDNITA, formed alongside HNO_3). ALKONITA and IDNITA are modeled after the existing IONITA (isoprene nitrate aerosol), and $INDIOL_N$ is given the same properties as INDIOL (the generic aerosol-phase organonitrate hydrolysis product). See Text S1 in the Supporting Information for details. Beyond this, we make no changes to the chemical mechanism in GEOS-Chem given that the goal of this work is to assess the existing budget of NO_y.

2.2 ATom Observations

The Atmospheric Tomography Mission (ATom)(Thompson et al., 2022; Wofsy et al., 2018, 2021) surveyed the composition of the remote atmosphere above the Atlantic and Pacific basins during four sets of flights (ATom-1 through ATom-4) between July 2016 and May 2018, sampling each season for approximately a month at a time (Fig. 1). The NASA DC-8 aircraft, which cyclically profiled the troposphere from ~0.2 to 12 km altitude, included instrumentation aboard to measure both gas and aerosol species. We use this multi-season campaign with its consistent vertical profiling to evaluate the global simulation of NO_y. Table 1 describes the measurements of NO, NO_2, HNO_3, and PAN used in this work. We sample the model for the time and location of all flights.

The NO_2 measurements can suffer at higher altitude from interferences from thermal decomposition of peroxynitric acid (HNO_4) and methyl peroxy nitrate (MPN) which may bias the NO_2 measurements (Bourgeois et al., 2022; Shah et al., 2023;

https://doi.org/10.5194/egusphere-2026-875
Preprint. Discussion started: 24 February 2026

Silvern et al., 2018; Travis et al., 2016). Following Shah et al. (2023) we therefore estimate NO_2 from the NO-NO_2 photostationary state (PSS):

$$NO + O_3 \longrightarrow NO_2 + O_2 \quad (R_1)$$

$$NO + HO_2 \longrightarrow NO_2 + OH \quad (R_2)$$

$$NO + RO_2 \longrightarrow NO_2 + RO \quad (R_3)$$

$$NO + BrO \longrightarrow NO_2 + Br \quad (R_4)$$

$$NO_2 + h\nu \xrightarrow{O_2} NO + O_3 \quad (R_5)$$

$$PSS = \frac{[NO]}{[NO_2]} = \frac{j_{NO2}}{k_1[O_3] + k_2[HO_2] + k_3[RO_2] + k_4[BrO]} \quad (1)$$

$$[\boldsymbol{NO_2}] = \frac{[\boldsymbol{NO}]}{\boldsymbol{PSS}} \quad (2)$$

For simplicity, we elect to use the Arrhenius parameterization for R_1, as only a small number of points (sampled above 9 km) fall outside the recommended range, and the two parameterizations differ by only 15% at these low temperatures. As in Shah et al. (2023), we use GEOS-Chem-simulated concentrations of species that were not measured or had insufficient coverage (HO_2, RO_2, and BrO) in our analysis, and treat the CH_3O_2 + NO reaction as a model for R_3, using rate constants from Burkholder et al. (2019). Species included within the GEOS-Chem definition of RO_2 are listed in Text S2 in the Supporting Information. We find that the PSS correction factor (Eq. 1) is dominated by the NO + O_3 reaction (R_1), as it accounts for 36-81% of the denominator. The NO + RO_2 and NO + HO_2 reactions (Eqs. R_2 and R_3) are of comparable importance and account for 11-40% and 2-27% respectively. The NO + BrO reaction (Eq. R_4) has a minor but non-negligible contribution (1-12%), peaking in the winter. Our model evaluation in Section 3.1 uses the PSS NO_2 vertical profiles (Eq. 2).

We remove ATom data that sampled fresh NO_x emissions (NO_y : NO < 3 mol mol^{-1}), early mornings and late evenings (solar zenith angle > 70°)(Shah et al., 2023), points that may have been influenced by stratospheric air masses (O_3 / H_2O > 1 ppbv $ppmv^{-1}$)(Bourgeois et al., 2021), and flights over continents. Additionally, we filtered out plumes, as they cannot be represented by the GEOS-Chem model (Rastigejev et al., 2010), by excluding the 97th percentile of data and above. Between 14-19% of the NO data remaining after filtering is below the lower end of the detection limit (5 ppt). We retain this fraction in order not to high bias the observations; however, we note that observational constraints on NO are less reliable at low concentrations. We compare the sum of NO, NO_2 (PSS-corrected), HNO_3, and PAN (ΣNO_y), the key contributors to NO_y, as in Murray et al., (2021), to our model. Sampling times with missing data for any one of these four constituents are not included in the model-observation comparison of NO_y. We exclude aerosol NO_3^- from our model evaluation as it accounts for on average 1-3% of NO_y and is often reported as below detection limit in the remote troposphere during ATom. A model-observation comparison of total NO_y from the NOAA-NOyO3 chemiluminescence instrument is available in Fig. S1 in the Supporting Information. Species included in the model definition of NO_y for this comparison are in Text S2. Additional NO_y species that were not measured consistently across ATom (e.g., peroxypropionyl nitrate (PPN), HNO_4, and N_2O_5) are also excluded from the main text, but we include a model-observation comparison for these species in Fig. S2 in the Supporting Information.

https://doi.org/10.5194/egusphere-2026-875
Preprint. Discussion started: 24 February 2026

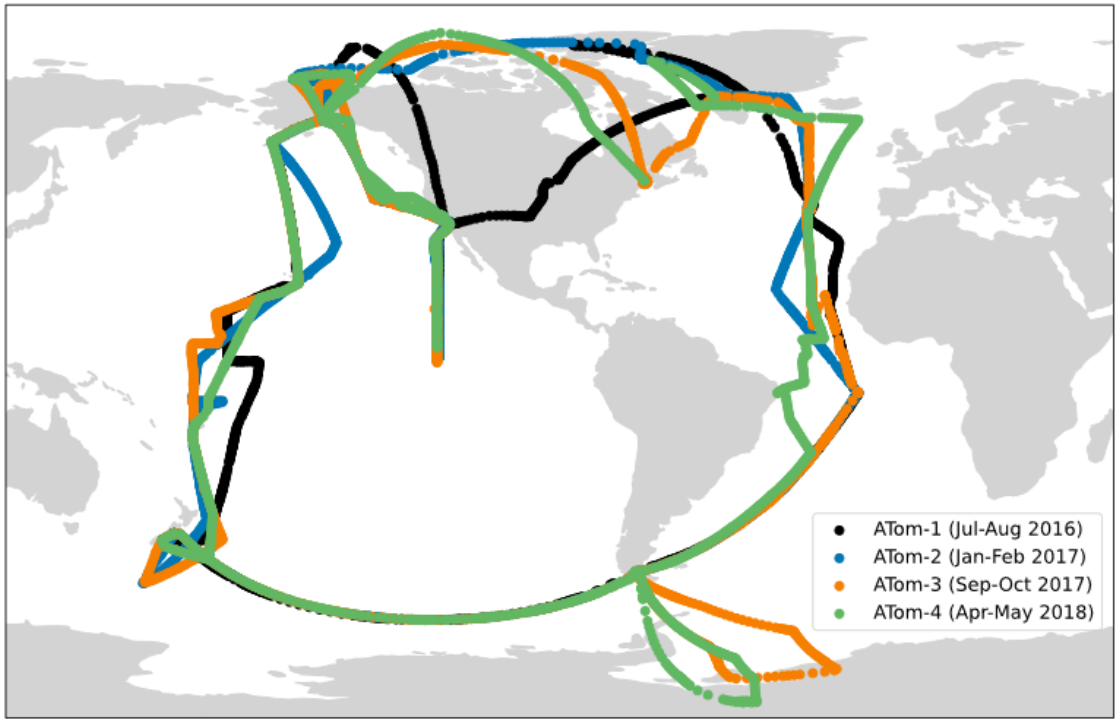

Figure 1: Flight tracks of the four deployments (see dates in legend) comprising the ATom field campaign.

200

Measurement	Instrument	Uncertainty	References
NO, NO_2, O_3, NO_y	NOAA NOy-O_3	NO: ± (5% + 6 pptv), NO_2: ± (7% + 20 pptv), NO_y: ± (12% + 10 pptv), O_3: ± (2% + 15 pptv)	Bourgeois et al. (2020, 2021); Ryerson et al., (2000, 2019)
HNO_3	CIT-CIMS	30%	Allen et al. (2021, 2022); Crounse et al. (2006)
PAN	NOAA PANTHER	10%	Moore et al. (2022)

Table 1: Description of ATom measurements used to evaluate the model simulation. For uncertainties given as ± (x% + y pptv), x represents the accuracy and y represents the 2σ precision in 1 s.

205

https://doi.org/10.5194/egusphere-2026-875
Preprint. Discussion started: 24 February 2026

3 Results

3.1 Model Evaluation using the ATom Campaign

Prior to describing the GEOS-Chem NO_y budget in detail, we present a simple global-scale model evaluation compared to the ATom measurements. These comparisons provide some context for uncertainties discussed in Sections 3.2. and 3.3.

Figure 2 shows a comparison of vertical profiles measured by the ATom campaign and those simulated by the model. The model captures the general shape of the ΣNO_y (= NO + NO_2 + HNO_3 + PAN) vertical profile throughout the troposphere, as well as the magnitude in the Southern Hemisphere. The model exhibits a high bias in the Northern Hemisphere throughout the year, except in the summer.

As discussed in Section 2.2, there is likely a high bias in the measurement of NO_2 aboard ATom. Fig. S1 in the Supporting Information shows the effect of applying the PSS correction factor to NO_2. We see that the native chemiluminescence measurements would indicate that the model consistently underestimates NO_x. However, application of the PSS correction leads to much better agreement between the model and observations across seasons, particularly in the southern hemisphere. Some positive and negative biases remain in the Northern Hemisphere (see Fig. S1 in the Supporting Information for details).

The model systematically overestimates HNO_3, a long-standing bias in GEOS-Chem (Norman et al., 2024; Travis et al., 2016; Zhang et al., 2012). It is also unable to capture the general shape of the HNO_3 vertical profile across seasons in both hemispheres. An alternative wet deposition scheme (Luo et al., 2019, 2020) is able to largely correct this high bias over the remote ocean (Travis et al., 2020). However, these updates are inconsistent with continental measurements of deposition made over the United States (Dutta and Heald, 2023). Thus, further investigation is needed to improve the HNO_3 simulation.

Although the model representation of PAN does have a moderate high bias, the shape of the vertical profile is reasonably well-captured across seasons. This is consistent with a previous model evaluation of PAN, which explored the sensitivity of PAN chemistry to spatially heterogeneous factors (the variety of VOC precursors, biomass burning in the remote high latitudes, and lightning as a source of NO_x at high altitudes)(Fischer et al., 2014). A comparison against additional measurements of PAN taken during ATom are included in Fig. S1 in the Supporting Information.

Overall, the model captures the amount and speciation of total NO_y measured during ATom best in the Southern Hemisphere (year-round) and in the Northern Hemisphere in the summer (Fig. S1 in the Supporting Information). Figure 2 shows that the model exhibits excess HNO_3 year-round throughout the column in the Northern Hemisphere, and in the free troposphere in the Southern Hemisphere. There is also excess model NO and PAN, to a lesser degree than HNO_3, in the Northern Hemisphere spring-fall. We present these comparisons as a benchmark for interpreting the global budgets that follow.

https://doi.org/10.5194/egusphere-2026-875
Preprint. Discussion started: 24 February 2026

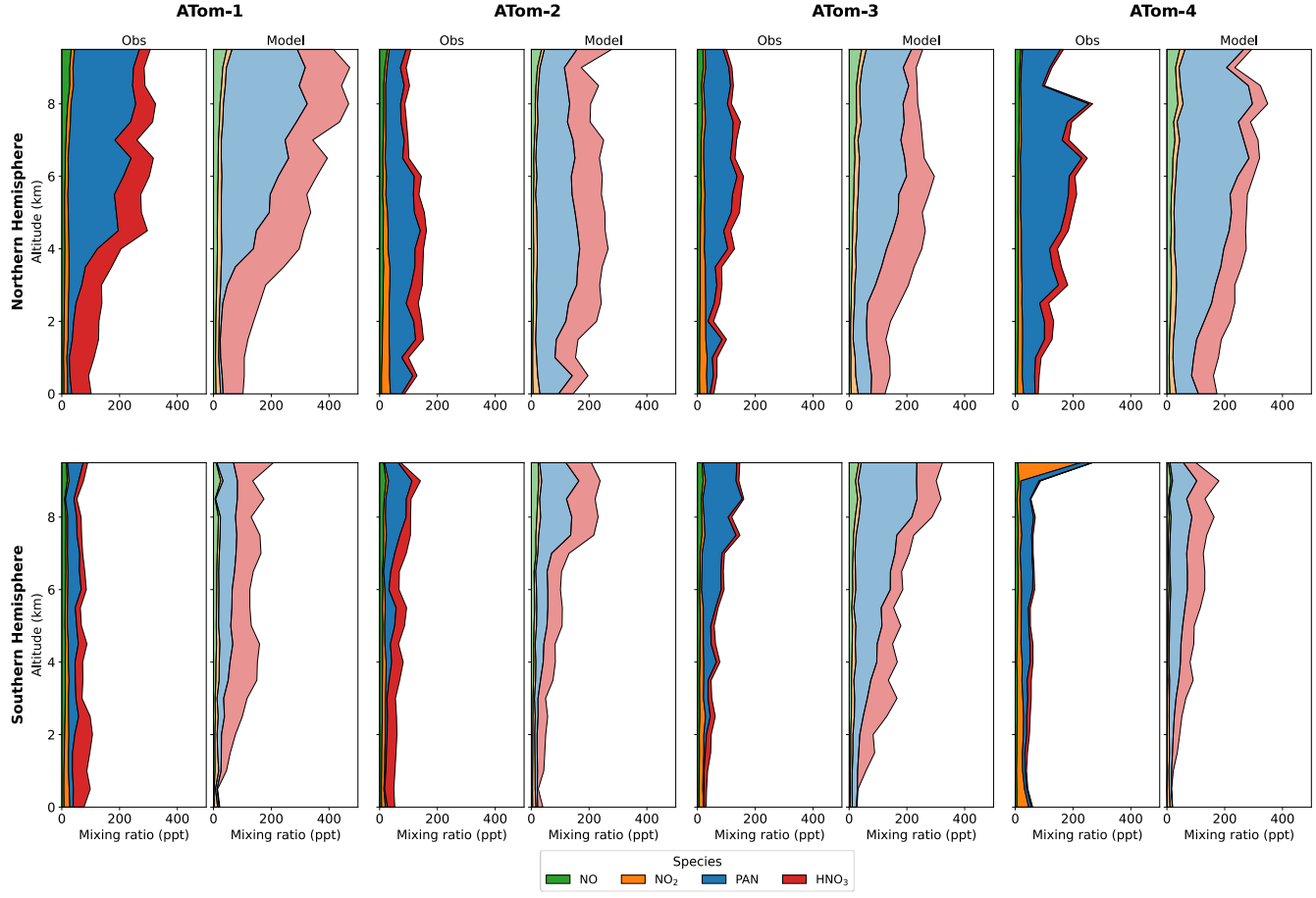

Figure 2: Observed (saturated) and modeled (desaturated colors) stacked median vertical profiles of ΣNO$_y$ during ATom flights, separated by Northern Hemisphere (top row) and Southern Hemisphere (bottom row). For a detailed comparison of all species, see Fig. S1 in the Supporting Information.

3.2 Global Budget of NO$_x$ and NO$_y$

The global burdens of various NO$_y$ species are set by an equilibrium between sources (emissions, chemical production) and sinks (wet and dry deposition, chemical loss). We characterize these sources and sinks based on a 2016 simulation; interannual variability in the total abundance of NO$_y$ is expected due to variations in natural sources (including fires) and removal via precipitation, but we expect the overall partitioning of NO$_y$ species presented here to be robust. Table 2 summarizes the major NO$_y$ emissions. These are dominated by NO$_x$ (~94%), with small quantities of HNO$_3$ (as a consequence of the parameterization of NO$_x$ chemistry from ship emissions plumes, discussed in Section 2.1) and alkyl nitrates making up the remainder. NO$_x$ is primarily emitted as NO (51 Tg N yr^{-1}), with a minor contribution from NO$_2$ (2.5 Tg N yr^{-1}). Anthropogenic sources (including here aircraft and ship) contribute 63% of NO$_x$ emissions (33.9 Tg N yr^{-1}), with fires, lightning, and soil contributing a little more than 10% each. Approximately 76% of these emissions are in the Northern Hemisphere.

https://doi.org/10.5194/egusphere-2026-875
Preprint. Discussion started: 24 February 2026

Species	Emissions (2016) (Tg N yr^{-1})	
NO_x	Total	53.5
	Anthropogenic	30.3
	Aircraft	0.9
	Ship	2.7
	Biomass burning	5.9
	Lightning	6.2
	Soil	7.4
HNO_3	Ship	3.1
Ethyl and methyl nitrate	Ocean	0.2

Table 2: Annual global emissions of NO_y species for 2016 from CEDS v2 in GEOS-Chem

Figure 3 shows a summary of the modeled annual global tropospheric budget of NO_y simulated for 2016. ΣPNs refers to peroxy nitrates, XNO_y is a catchall for halogen nitrates and nitrites, orgNIT includes both gas-phase organic nitrates and related nitrogen-containing peroxy and alkoxy radicals, and NO_3^- is comprised of both fine (NIT) and coarse (NITs) mode particulate nitrates. See Text S3 in the Supporting Information for the complete lists of model species that define each of these families. Emissions are shown as vertical red arrows, with deposition shown as vertical blue and yellow arrows. All chemical fluxes that exceed 1 Tg N yr^{-1} are shown as light blue arrows, except for those that represent radical cycling between NO, NO_2 and NO_3 (discussed in greater detail in Section 3.3). The total burden of NO_y is 858 Gg N, with major contributions from NO_x (134 Gg N), HNO_3 (303 Gg N), fine and coarse aerosol NO_3^- (90 Gg N and 11 Gg N respectively), and ΣPNs (254 Gg N) (of which PAN is the major component, corresponding to 205 Gg N, followed by PPN = 38 Gg N, and MPN = 10 Gg N). The deposition of HNO_3 and NO_3^- (51.9 Tg N yr^{-1}) is responsible for 90% of NO_y deposition (57.4 Tg N yr^{-1}) and therefore governs the lifetime of NO_y (τ_{dep} ~ 5.5 days). The total NO_y deposition is slightly higher than the total emissions (56.8 Tg N yr^{-1}). This is due to a small net input of nitrogen in the form of nitric acid from the stratosphere ~0.6 Tg N yr^{-1}, as seen in ACCMIP (Lamarque et al., 2013). The tropospheric lifetime of HNO_3 to deposition is ~2.9 days, with approximately equal contributions from wet and dry deposition. We further discuss the chemical fluxes amongst key species in Section 3.3. A more detailed version of this budget is available in Table S3 in the Supporting Information.

https://doi.org/10.5194/egusphere-2026-875
Preprint. Discussion started: 24 February 2026

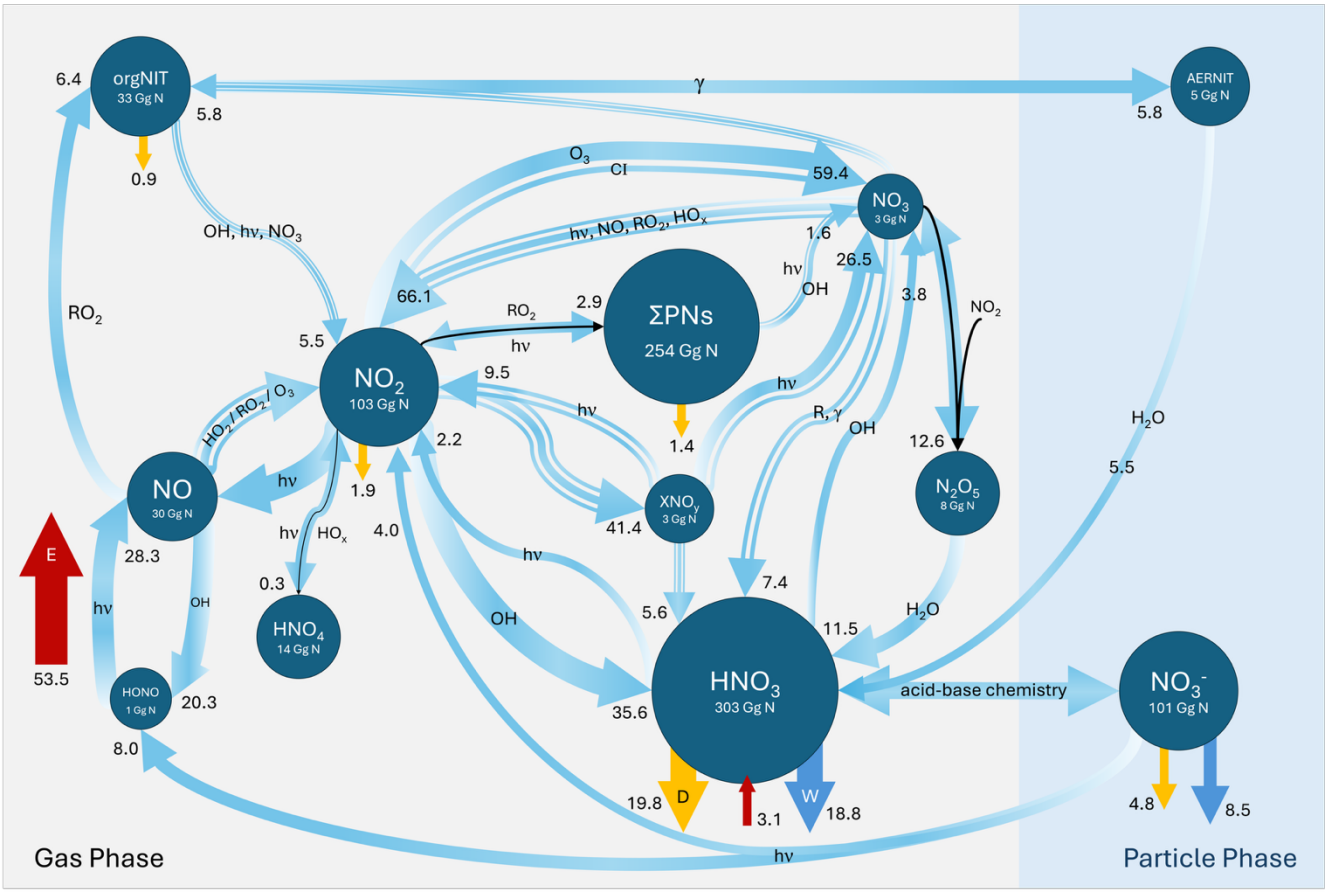

Figure 3: Modeled NO_y budget for 2016 showing key species and families (dark blue circles) in Gg N. Chemical fluxes exceeding 1 Tg N yr^{-1} are represented by curved light blue arrows. Compound arrows indicate where multiple flux pathways between species have been lumped. Net fluxes between species that undergo rapid cycling are shown with inset curved black arrows. Physical fluxes exceeding 0.5 Tg N yr^{-1} are represented by vertical arrows and include emissions (red arrows), wet deposition (blue arrows), and dry deposition (yellow arrows).

Figure 4 shows the concentrations of NO_x and NO_y, as well as their ratio of at the surface and at 500 hPa. High NO_x:NO_y regions near the surface are indicative of fresh NO_x emissions, with the peaks near urban centers, major shipping lanes, and biomass burning regions. At the surface, the global average ratio of NO_x:NO_y is 0.23, and over continents it is 0.34. In the free troposphere, much of the NO_x is consumed to form longer-lived NO_z (= NO_y – NO_x), with a low, diffuse NO_x:NO_y ratio reflecting long-range transport and mixing. At 500 hPa, both NO_x and NO_y concentrations are lower, and the ratio is more spatially homogenous, with the continental average being within 5% of the global average of 0.10. Regions with high NO_x:NO_y ratios aloft, such as those seen in the tropics, are primarily due to lightning NO_x emissions.

https://doi.org/10.5194/egusphere-2026-875
Preprint. Discussion started: 24 February 2026

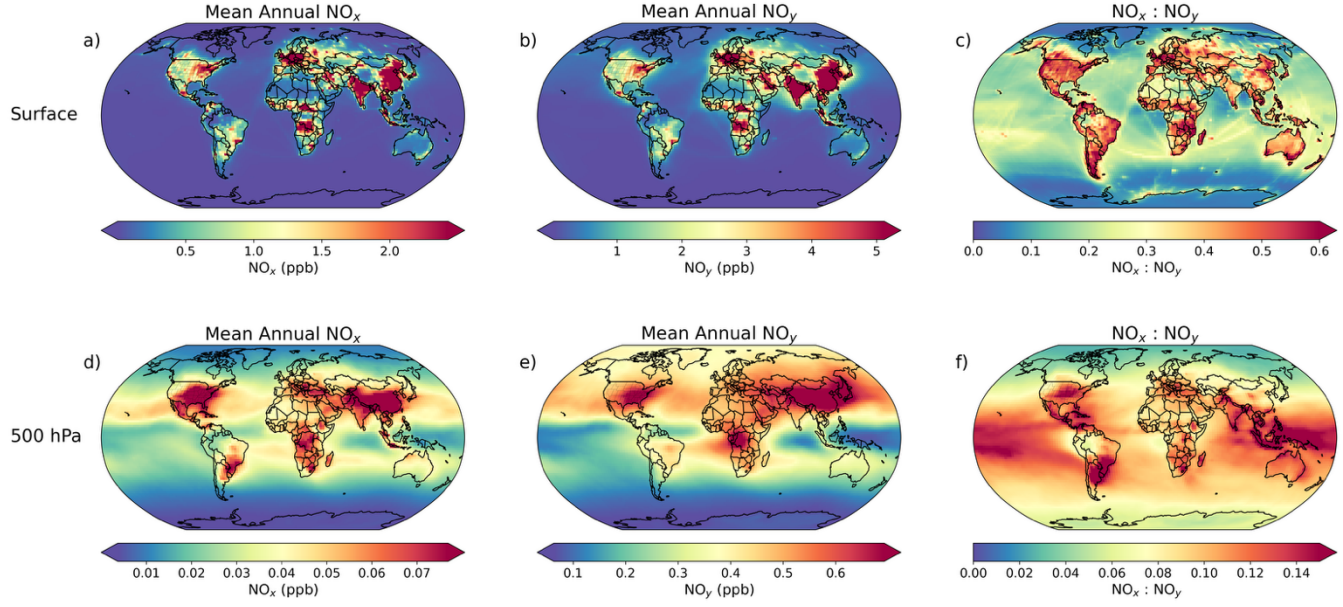

Figure 4: GEOS-Chem simulation of annual mean (2016) concentrations of NO_x (ppb), NO_y (ppb) and NO_x : NO_y at (a-c) the surface and (d-f) 500 hPa. See Text S4 in the Supporting Information for species included in the model definition of NO_y.

As described in Section 1, NO_x undergoes rapid chemical cycling with a number of other NO_y species (NO_3, HONO, HNO_4, N_2O_5, ΣPNs). However, the primary sink of NO_x is the formation of nitric acid (HNO_3), with approximately 36.2 Tg N yr^{-1} formed from NO_2. Given rapid cycling of NO_x with ΣPNs, and HONO, the resulting mean global chemical lifetime for NO_x is ~44 min. However, if we exclude rapid cycling and instead only consider net loss of NO_x, the mean global chemical lifetime of NO_x is ~21 hours.

3.3 NO_y Chemical Cycling

Figure 3 summarizes the main chemical and physical flows within the NO_y family. Here we discuss in further detail the budgets of key reservoir species within that family. Table S2 provides all annual mean simulated fluxes for each reaction, based on definitions of families described in Text S3 in the Supporting Information.

Figure 5 summarizes the budget of total nitrate (TNO_3 = HNO_3 + pNO_3^-). As described above, the main source of HNO_3 is production via NO_2 (36.2 Tg N yr^{-1}), most (98%) of which is formed by the oxidation of NO_2 by OH (35.6 Tg N yr^{-1}) with a minor (2%) contribution from aerosol uptake of NO_2 (0.5 Tg N yr^{-1}). Heterogeneous chemistry that includes N_2O_5 hydrolysis (11.5 Tg N yr^{-1}, of which 2.2 Tg N yr^{-1} is from cloud uptake) and uptake by sea salt (0.4 Tg N yr^{-1}) is the second most important source of HNO_3. Aerosol uptake of NO_3 (3.0 Tg N yr^{-1}) and the production of HNO_3 as a byproduct of RO_2 formation by NO_3 (4.4 Tg N yr^{-1}) are minor sources of HNO_3. Other sources include halogen nitrate uptake on sea salt, hydrolysis, or breakdown by acids (e.g. HCl, HBr) (5.6 Tg N yr^{-1}), and aerosol nitrate hydrolysis (5.5 Tg N yr^{-1}).

https://doi.org/10.5194/egusphere-2026-875
Preprint. Discussion started: 24 February 2026

As discussed previously, almost all NO_y removal from the troposphere is via deposition of HNO_3 (38.6 Tg N yr^{-1}). In GEOS-Chem, the equilibrium partitioning of HNO_3 between gas and particle phase NO_3^- is calculated by ISORROPIA II, and therefore we can estimate the net formation of NO_3^- from HNO_3 to be 25 Tg N yr^{-1} – 13.4 Tg N yr^{-1} as fine mode nitrate aerosol (NIT), and 11.6 Tg N yr^{-1} as coarse mode aerosol (NITs). Other losses of HNO_3 include oxidation by OH to form NO_3 (3.8 Tg N yr^{-1}), photolysis to form NO_2 (2.2 Tg N yr^{-1}), and uptake of HNO_3 on sea salt to form coarse mode aerosol inorganic nitrate (0.3 Tg N yr^{-1}, not shown in Fig. 5). While pNO_3^- was classically treated to be a terminal sink for NO_x, recent implementation of NO_x recycling via photolysis of pNO_3^- to form HONO and NO_2 implies that NO_3^- now serves as a reservoir species. In our model representation, this photolysis is non-negligible (12.0 Tg N yr^{-1}), with approximately 8.0 Tg N yr^{-1} forming HONO (which rapidly cycles with NO during the daytime), and 4.0 Tg N yr^{-1} being recycled directly back to NO_2. This is comparable to the total deposition of pNO_3^- (13.3 TgN yr^{-1}).

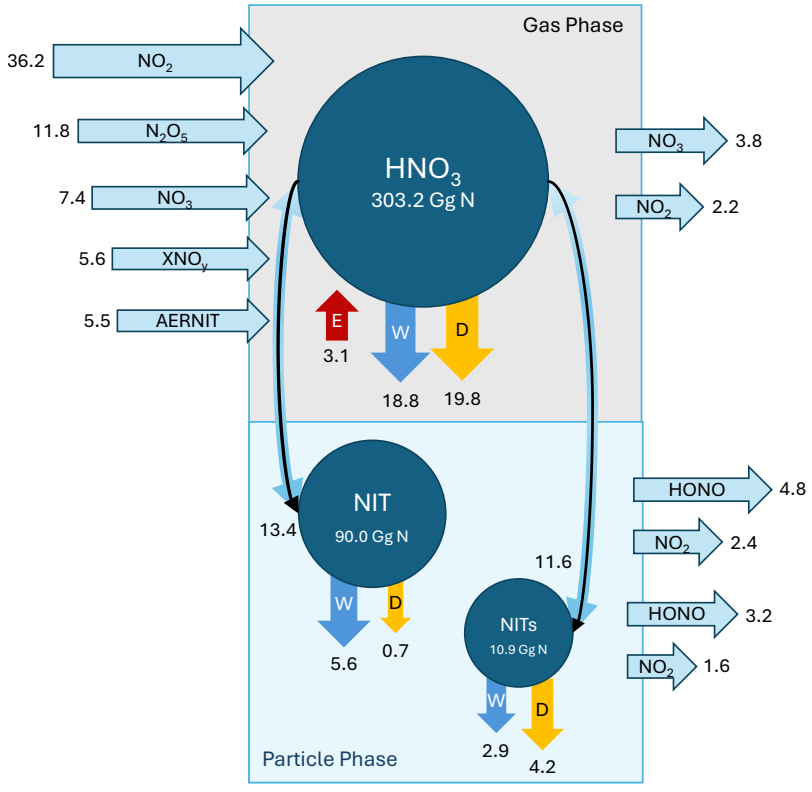

Figure 5: Summary of annual TNO_3 budget in GEOS-Chem for 2016, showing sources (red), chemical fluxes (light blue), and wet (blue) and dry (yellow) deposition. Here NIT are fine mode nitrate aerosol and NITs are coarse mode nitrate aerosol.

Peroxy nitrates (ΣPNs) are the other major reservoir species. They are formed near the surface where NO_x is abundant and RO_2 readily forms from the oxidation of volatile organic compounds (VOCs) by OH. ΣPNs are stable at lower temperatures in the free troposphere and therefore able to transport NO_y away from NO_x source regions. As air masses descend, warmer

https://doi.org/10.5194/egusphere-2026-875
Preprint. Discussion started: 24 February 2026

temperatures lead to ΣPN decomposition, releasing NO_x downwind of sources. In the model, there is rapid formation and decomposition of ΣPNs (formation = 811.3 Tg N yr^{-1}, loss = 810.0 Tg N yr^{-1}). Of these, the rate of production and loss of MPN is the fastest (production = 654.8 Tg N yr^{-1}, loss = 654.9 Tg N yr^{-1}, of which 0.8 Tg N yr^{-1} is by photolysis), followed by PAN (production = 132.4 Tg N yr^{-1}, loss = 130.7 Tg N yr^{-1}, of which 1.2 Tg N yr^{-1} is by photolysis). There is a net production (2.9 Tg N yr^{-1}) of ΣPNs from NO_2, and there is a net loss of ΣPNs to form NO_3 via oxidation by OH (1.1 Tg N yr^{-1}) and photolysis (0.5 Tg N yr^{-1}). Approximately 1.5 Tg N yr^{-1} of ΣPNs are lost by deposition, primarily via dry deposition.

Figure 6 summarizes the budget of organic nitrates, the representation of which is highly simplified in GEOS-Chem. Organic nitrates are formed primarily by the oxidation of NO by peroxy radicals (6.4 Tg N yr^{-1}) and oxidation of BVOCs by the nitrate radical (5.8 Tg yr^{-1}). Alkyl nitrates (ALKNIT) represent a majority of the gas-phase organic nitrate burden (27.5 Gg N), followed by isoprene nitrates (ISOPNIT) (2.9 Gg N), monoterpene nitrates (MTNIT) (1.0 Gg N), and other short-chain nitrates (C_3NIT) (1.0 Gg N). Only a small fraction of the total gas phase organic nitrate loss is accounted for by deposition (1.2 Tg N yr^{-1}). Instead, once formed, these lumped gas-phase nitrates (including those formed from the oxidation of isoprene, monoterpenes, and alkyl nitrates) either recycle NO_x as NO_2 (5.5 Tg N yr^{-1}), or are subject to aerosol uptake that represents the formation of particulate matter (5.8 Tg N yr^{-1}), neglecting more complex processes. The formation of particle-phase organic nitrates (AERNIT) (mean annual burden of 5 Gg N) is dominated by ISOPNIT (56%), followed by MTNIT (20%), ALKNIT (19%), and aromatics (5%). Once formed, AERNITs rapidly hydrolyse to form HNO_3 (5.5 Tg N yr^{-1}), which vastly outcompetes their deposition (0.4 Tg N yr^{-1}).

Almost all alkyl nitrate formation (93%) occurs via the RO_2 + NO pathway. Once formed, the losses are via aerosol uptake (48%), NO_x recycling (38%), and deposition (14%). In contrast, only 56% of isoprene nitrates are formed by this pathway, with 41% accounted for by the oxidation of isoprene initiated by NO_3. Despite the differences in formation, the fate of isoprene nitrates is similar to that of alkyl nitrates, with 45% forming aerosol nitrate, 38% recycling NO_2, 8% removed by deposition, and the remaining 7% forming shorter-chain organic nitrates (C3NIT)(primarily via reaction with HO_2 or NO, and with small contributions from photolysis or reaction with OH). These C3NIT are formed either from isoprene-derived precursors (44%) or by the oxidation of short-chain VOCs (methacrolein or lumped >C3 alkenes) by NO_3 (40%) and are removed primarily by photolysis (54%) or NO- or RO_2-mediated reactions, both of which form NO_2 (25%). Deposition contributes 14% of the loss of C3NIT.

Monoterpene chemistry is simplified to a greater degree than isoprene chemistry in GEOS-Chem. 85% of monoterpene nitrates are formed from the oxidation of monoterpenes by NO_3, while only 15% are formed via RO_2 + NO. However, the fate of monoterpene nitrates closely mirrors that of isoprene nitrates, with 48% forming organic aerosol, 44% recycling to NO_2, and 8% removed by deposition.

https://doi.org/10.5194/egusphere-2026-875
Preprint. Discussion started: 24 February 2026

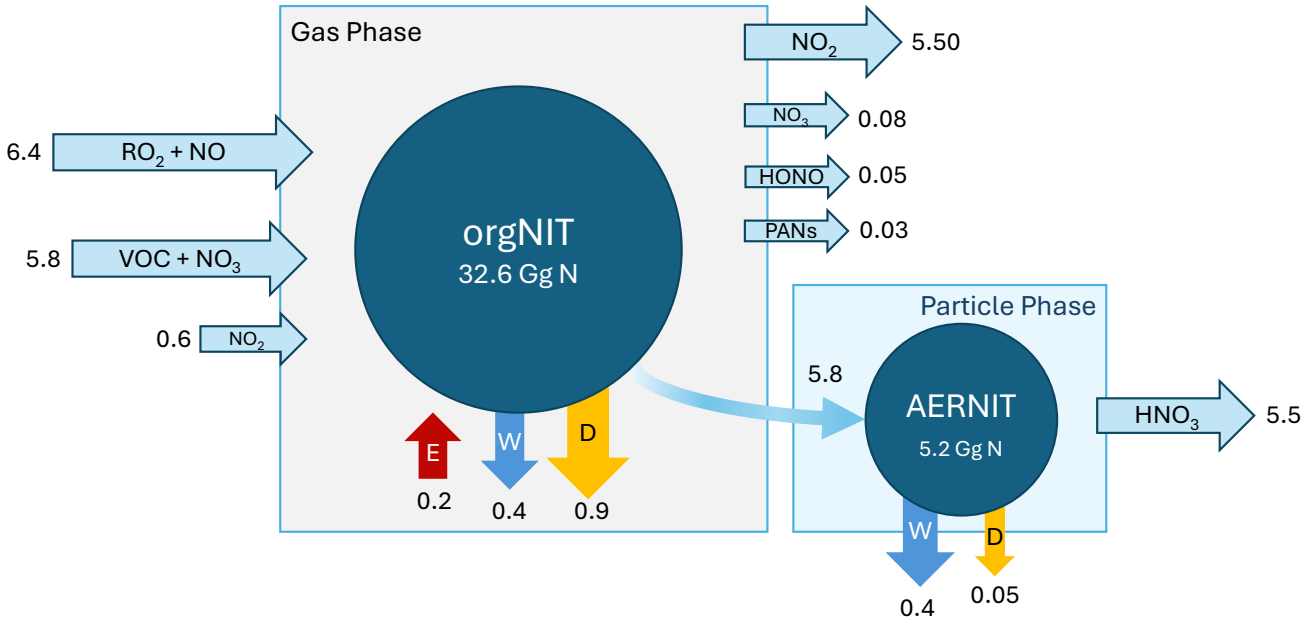

Figure 6: Summary of annual organic nitrate budget in GEOS-Chem for 2016, showing sources (red), chemical fluxes (light blue), and wet (blue) and dry (yellow) deposition.

HONO can function as an important source of OH radicals in the morning (Section 1). The major sources of HONO are the oxidation of NO by OH (20.3 Tg N yr^{-1}) and the photolysis of particulate inorganic nitrate (pNO_3^-)(8.0 Tg N yr^{-1}), with a minor contribution from NO_2 uptake on aerosol surfaces (0.5 Tg N yr^{-1}). Almost all HONO (98%) is photolyzed during the day to form NO and OH (28.3 Tg N yr^{-1}), while the remainder is further oxidized by OH to form NO_2 and water.

The nitrate radical (NO_3) is the key driver of nighttime tropospheric NO_y chemistry. It is formed primarily by the oxidation of NO_2 by O_3 (52.2 Tg N yr^{-1}), and the decomposition of halogen nitrates (25.1 Tg N yr^{-1} by photolysis, and 1.4 Tg N yr^{-1} by miscellaneous oxidants). Smaller sources of NO_3 include the oxidation of HNO_3 and peroxymethacroyl nitrate (MPAN) by OH (3.8 Tg N yr^{-1} and 1.1 Tg N yr^{-1} respectively), and the photolysis of PAN (0.5 Tg N yr^{-1}) and N_2O_5 (forming 0.6 Tg N yr^{-1} each of NO_2 and NO_3). NO_3 forms NO_2 by photolysis (46.2 Tg N yr^{-1}), reaction with NO (14.5 Tg N yr^{-1}), reaction with RO_2 (3.7 Tg N yr^{-1}), or HO_x cycling (1.6 Tg N yr^{-1}); and forms NO by photolysis (6.0 Tg N yr^{-1}). It may form HNO_3 via oxidation of unsaturated VOCs (4.4 Tg N yr^{-1}) or via uptake on aerosol surfaces (3.0 Tg N yr^{-1}) and is responsible for 45% of the formation of organic nitrates (5.8 Tg N yr^{-1}).

N_2O_5 is formed entirely via the pressure-dependent bimolecular reaction between NO_2 and NO_3 (1037.5 Tg N yr^{-1} of N_2O_5, returning 511.9 Tg N yr^{-1} each to NO_2 and NO_3 upon decomposition. Some of this formation is balanced by a photolytic loss (0.6 Tg N yr^{-1} each to NO_2 and NO_3), giving a net formation of N_2O_5 of 12.6 Tg N yr^{-1}. There are additional losses to HNO_3 via hydrolysis (11.5 Tg N yr^{-1}) and uptake on sea salt (0.7 Tg N yr^{-1}), the latter of which also produces $ClNO_3$ in equal quantities. Deposition is a minor sink of N_2O_5 (0.4 Tg N yr^{-1} of dry deposition).

https://doi.org/10.5194/egusphere-2026-875
Preprint. Discussion started: 24 February 2026

As seen in Fig. 3, halogens play a central role in mediating the flow of reactive nitrogen between different NO_y species. XNO_y species are largely formed by the reaction of NO_2 with halogen atoms or halogen monoxides (41.4 Tg N yr^{-1}). These species are relatively short-lived and may decompose to form NO_3 (26.5 Tg N yr^{-1}, 95% of which is by photolysis) or NO_2 (9.5 Tg N yr^{-1}, 56% of which is by photolysis) or undergo uptake onto sea salt to form HNO_3 (5.6 Tg N yr^{-1}). Deposition of XNO_y is negligible (0.1 Tg N yr^{-1}, 86% of which is dry deposition).

4 Discussion and Conclusions

Nitrogen oxides have long been studied due to their central role in driving tropospheric chemistry. In this study, we characterize the global tropospheric budget for NO_y as represented in the GEOS-Chem chemical transport model. We also provide model estimates of the relative importance of the different chemical processes that control the production and loss of NO_y species in the global troposphere. As discussed in Section 2.1, the earliest models of NO_y considered only a handful of reservoir species for NO_x (HONO, HNO_3, N_2O_5, and later PAN) (Levy II, 1972; Logan, 1983). Now, especially with advances in our understanding of organic nitrates and heterogeneous chemistry, we represent a more diverse array of reservoirs that transport NO_x further away from source regions into the remote troposphere. However, modern chemical transport models disagree on the abundance and speciation of this more complicated (and variable) representation of NO_y.

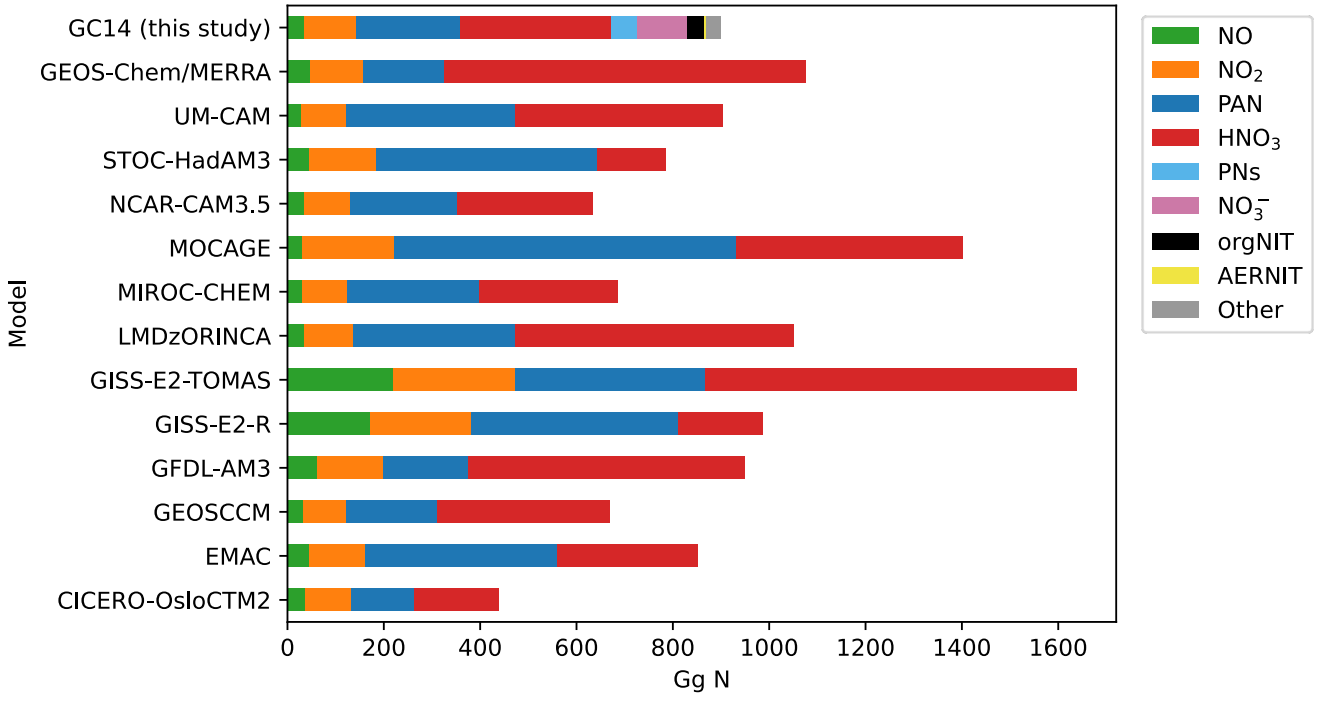

Figure 7: Decadal-average (2000s) global tropospheric burdens of the four major NO_y species across ACCMIP models (data from Murray et al., 2021) compared with NO_y burdens (including additional species) from this study (GC14) for 2016.

https://doi.org/10.5194/egusphere-2026-875
Preprint. Discussion started: 24 February 2026

Figure 7 shows the decadal-average burdens of four key NO_y species (NO, NO_2, HNO_3, and PAN) across ACCMIP models for the 2000s from Murray et al., (2021), compared to a more comprehensive set of results from our simulation of 2016 (GC14). The tropospheric burdens of the sum of these four NO_y species varies between models by a factor of 3.7. There is similarly large variation in speciation, with no clear trend between models. Murray et al. (2021) note numerous reasons for this variation that lead either directly to changes in NO_y lifetime by physical removal, or indirectly by reactive loss due to differences in oxidant abundance, as well as differences in the spatial distribution of lightning NO_x. Different implementations of heterogeneous chemistry across models are another source of uncertainty (e.g., some models consider variations in reactive uptake based on aerosol composition while others do not), thereby altering local sinks of NO_y. Finally, models vary in their representation of the competition between reactive loss and physical loss (which is also the case for reactive carbon) and the degree to which they permit NO_x recycling from reservoirs.

Despite advances in our understanding of NO_y chemistry over the last 70 years, there remain numerous uncertainties in our ability to accurately represent the global abundances of many NO_y species in models. In Section 1, we noted the GEOS-Chem model's long-standing overestimate of HNO_3. However, Fig. 7 shows that some ACCMIP models exhibit even higher HNO_3 than GEOS-Chem, suggestive of wide-spread issues in the simulation HNO_3 and potentially the need for additional chemical loss pathways. Additionally, our understanding of pNO_3^- as a terminal sink for NO_y has been challenged in recent years – renoxification by photolysis allows pNO_3^- to act as a reservoir for NO_y instead. However, the efficiency of this renoxification is still uncertain and will require coordinated model, lab, and field studies to constrain.

In Section 3.3 we characterize the impact of organic chemistry on NO_y cycling. This is an area of study that is rapidly evolving, and updates to the model's representation of organic chemistry, especially monoterpene chemistry, will likely lead to changes to the NO_y budget. We also find that deposition is presently a relatively small sink for organic nitrates in the model, given the large (and perhaps excessive) hydrolysis loss. Constraints on organic nitrogen deposition are limited; one study suggests that wet deposition of organic nitrogen in Rocky Mountain National Park is comparable to that of nitrate (Beem et al., 2010). Thus, the balance between chemical and physical losses requires more attention. In service of this, we advocate for additional collocated measurements of both concentrations and deposition, with a characterization of organic and inorganic NO_y. However, we note that modifications to the current balance between reactive and physical loss of aerosol organic nitrate will likely have minimal impacts on the high model HNO_3 bias, as this hydrolysis represents only ~8% of HNO_3 sources.

There have also been recent changes to the model's representation of halogen chemistry, which is another active area of research in the troposphere. The systematic approach to characterizing not just burdens and physical sinks but also chemical cycling used in this study may enable efforts to probe the sensitivity of the NO_y system to changes in chemistry or future emissions.

We have provided a summary of the global tropospheric NO_y budget for a single year and at monthly mean timescales. Future exploration of the NO_y budget on diurnal and seasonal timescales is needed. Additionally, while the focus of this

https://doi.org/10.5194/egusphere-2026-875
Preprint. Discussion started: 24 February 2026

study was to examine NO_y on a global scale, we acknowledge that the relative importance of different NO_y interconversion pathways could vary considerably at the regional scale. Finally, this study represents only a single model's characterization of global NO_y chemistry. As discussed previously, there is a range of complexity represented across different global chemistry models, and a comparison of NO_y fluxes across models would help us further understand the processes that give rise to differences in burdens and speciation.

Data Availability

The data that support the findings of this study are available on Zenodo (Dutta et al., 2026).
Observational data for the ATom campaign data are publicly available at: https://espo.nasa.gov/atom (last access: 1 March 2025)(ATom, 2025).
The GEOS-Chem model is publicly available at https://doi.org/10.5281/zenodo.10640536 (GEOS-Chem v14.3.0, 2024).

Author Contributions

ID and CLH designed the study. ID performed the simulations and led the analysis. EJH and FLM provided measurements of PAN used in the analysis. JDC provided measurements of HNO_3 used in the analysis. IB and JP provided measurements of NO_y, NO, and NO_2, and O_3 used in the analysis. ID and CLH wrote and edited the paper with input from all co-authors.

Competing Interests

The authors declare that they have no conflicts of interest.

Acknowledgements

We acknowledge the following investigators for providing measurements of NO, NO_2, NO_y, O_3, HNO_3, HNO_4, PPN, PAN, NO_3^-, N_2O_5, $ClNO_2$, and water vapor: Hannah M. Allen, Pedro Campuzano-Jost, Douglas A. Day, Joshua P. DiGangi, Glenn S. Diskin, Geoffrey S. Dutton, James W. Elkins, Bradley D. Hall, L. Gregory Huey, Jose L. Jimenez, Michelle J. Kim, Saewung Kim, J. David Nance, Benjamin A. Nault, J. Andrew Neuman, John B. Nowak, Derek J. Price, Thomas B. Ryerson, Jason C. Schroder, David J. Tanner, Alexander P. Teng, Chelsea R. Thompson, Patrick R. Veres, and Paul O. Wennberg.
The model simulations and analyses presented here were conducted using the "Svante" cluster, a facility located at MIT's Massachusetts Green High Performance Computing Center and supported by the Center for Sustainability Science and Strategy (https://cs3.mit.edu).

https://doi.org/10.5194/egusphere-2026-875
Preprint. Discussion started: 24 February 2026

Financial Support

This study was supported by a National Science Foundation Division of Atmospheric and Geospace Sciences grant (AGS-2223070) to CLH at MIT. The Caltech group was supported by the National Aeronautics and Space Administration (NNX15AG61A, 80NSSC21K1704). EJH and FLM were partially supported by NASA award NNH17AE26I. IB and JP were partially supported by the NOAA cooperative agreements with CIRES, NA17OAR4320101 and NA22OAR4320151.

References

Akimoto, H., Takagi, H., and Sakamaki, F.: Photoenhancement of the nitrous acid formation in the surface reaction of nitrogen dioxide and water vapor: Extra radical source in smog chamber experiments, International Journal of Chemical Kinetics, 19, 539–551, https://doi.org/10.1002/kin.550190606, 1987.

Allen, H. M., Crounse, J. D., Kim, M. J., Teng, A. P., Xu, L., and Wennberg, P. O.: ATom: In Situ Data from Caltech Chemical Ionization Mass Spectrometer (CIT-CIMS), V2, https://doi.org/10.3334/ORNLDAAC/1927, 2021.

Allen, H. M., Crounse, J. D., Kim, M. J., Teng, A. P., Ray, E. A., McKain, K., Sweeney, C., and Wennberg, P. O.: H2O2 and CH3OOH (MHP) in the Remote Atmosphere: 1. Global Distribution and Regional Influences, Journal of Geophysical Research: Atmospheres, 127, e2021JD035701, https://doi.org/10.1029/2021JD035701, 2022.

Amos, H. M., Jacob, D. J., Holmes, C. D., Fisher, J. A., Wang, Q., Yantosca, R. M., Corbitt, E. S., Galarneau, E., Rutter, A. P., Gustin, M. S., Steffen, A., Schauer, J. J., Graydon, J. A., Louis, V. L. S., Talbot, R. W., Edgerton, E. S., Zhang, Y., and Sunderland, E. M.: Gas-particle partitioning of atmospheric Hg(II) and its effect on global mercury deposition, Atmospheric Chemistry and Physics, 12, 591–603, https://doi.org/10.5194/acp-12-591-2012, 2012.

Andersen, S. T., Carpenter, L. J., Reed, C., Lee, J. D., Chance, R., Sherwen, T., Vaughan, A. R., Stewart, J., Edwards, P. M., Bloss, W. J., Sommariva, R., Crilley, L. R., Nott, G. J., Neves, L., Read, K., Heard, D. E., Seakins, P. W., Whalley, L. K., Boustead, G. A., Fleming, L. T., Stone, D., and Fomba, K. W.: Extensive field evidence for the release of HONO from the photolysis of nitrate aerosols, Science Advances, 9, eadd6266, https://doi.org/10.1126/sciadv.add6266, 2023.

ATom: Atmospheric Tomography (ATom) | ESPO Data Archive, 2025.

Baergen, A. M. and Donaldson, D. J.: Photochemical Renoxification of Nitric Acid on Real Urban Grime, Environ. Sci. Technol., 47, 815–820, https://doi.org/10.1021/es3037862, 2013.

Bates, K. H. and Jacob, D. J.: A new model mechanism for atmospheric oxidation of isoprene: global effects on oxidants, nitrogen oxides, organic products, and secondary organic aerosol, Atmospheric Chemistry and Physics, 19, 9613–9640, https://doi.org/10.5194/acp-19-9613-2019, 2019.

Bates, K. H., Jacob, D. J., Li, K., Ivatt, P. D., Evans, M. J., Yan, Y., and Lin, J.: Development and evaluation of a new compact mechanism for aromatic oxidation in atmospheric models, Atmospheric Chemistry and Physics, 21, 18351–18374, https://doi.org/10.5194/acp-21-18351-2021, 2021.

Bates, K. H., Burke, G. J. P., Cope, J. D., and Nguyen, T. B.: Secondary organic aerosol and organic nitrogen yields from the nitrate radical (NO_3) oxidation of alpha-pinene from various RO_2 fates, Atmospheric Chemistry and Physics, 22, 1467–1482, https://doi.org/10.5194/acp-22-1467-2022, 2022.

https://doi.org/10.5194/egusphere-2026-875
Preprint. Discussion started: 24 February 2026

Bian, H., Chin, M., Hauglustaine, D. A., Schulz, M., Myhre, G., Bauer, S. E., Lund, M. T., Karydis, V. A., Kucsera, T. L., Pan, X., Pozzer, A., Skeie, R. B., Steenrod, S. D., Sudo, K., Tsigaridis, K., Tsimpidi, A. P., and Tsyro, S. G.: Investigation of global particulate nitrate from the AeroCom phase III experiment, Atmospheric Chemistry and Physics, 17, 12911–12940, https://doi.org/10.5194/acp-17-12911-2017, 2017.

Bourgeois, I., Peischl, J., Thompson, C. R., Aikin, K. C., Campos, T., Clark, H., Commane, R., Daube, B., Diskin, G. W., Elkins, J. W., Gao, R.-S., Gaudel, A., Hintsa, E. J., Johnson, B. J., Kivi, R., McKain, K., Moore, F. L., Parrish, D. D., Querel, R., Ray, E., Sánchez, R., Sweeney, C., Tarasick, D. W., Thompson, A. M., Thouret, V., Witte, J. C., Wofsy, S. C., and Ryerson, T. B.: Global-scale distribution of ozone in the remote troposphere from the ATom and HIPPO airborne field missions, Atmospheric Chemistry and Physics, 20, 10611–10635, https://doi.org/10.5194/acp-20-10611-2020, 2020.

Bourgeois, I., Peischl, J., Neuman, J. A., Brown, S. S., Thompson, C. R., Aikin, K. C., Allen, H. M., Angot, H., Apel, E. C., Baublitz, C. B., Brewer, J. F., Campuzano-Jost, P., Commane, R., Crounse, J. D., Daube, B. C., DiGangi, J. P., Diskin, G. S., Emmons, L. K., Fiore, A. M., Gkatzelis, G. I., Hills, A., Hornbrook, R. S., Huey, L. G., Jimenez, J. L., Kim, M., Lacey, F., McKain, K., Murray, L. T., Nault, B. A., Parrish, D. D., Ray, E., Sweeney, C., Tanner, D., Wofsy, S. C., and Ryerson, T. B.: Large contribution of biomass burning emissions to ozone throughout the global remote troposphere, Proceedings of the National Academy of Sciences, 118, e2109628118, https://doi.org/10.1073/pnas.2109628118, 2021.

Bourgeois, I., Peischl, J., Neuman, J. A., Brown, S. S., Allen, H. M., Campuzano-Jost, P., Coggon, M. M., DiGangi, J. P., Diskin, G. S., Gilman, J. B., Gkatzelis, G. I., Guo, H., Halliday, H. A., Hanisco, T. F., Holmes, C. D., Huey, L. G., Jimenez, J. L., Lamplugh, A. D., Lee, Y. R., Lindaas, J., Moore, R. H., Nault, B. A., Nowak, J. B., Pagonis, D., Rickly, P. S., Robinson, M. A., Rollins, A. W., Selimovic, V., St. Clair, J. M., Tanner, D., Vasquez, K. T., Veres, P. R., Warneke, C., Wennberg, P. O., Washenfelder, R. A., Wiggins, E. B., Womack, C. C., Xu, L., Zarzana, K. J., and Ryerson, T. B.: Comparison of airborne measurements of NO, NO_2, HONO, NO_y, and CO during FIREX-AQ, Atmospheric Measurement Techniques, 15, 4901–4930, https://doi.org/10.5194/amt-15-4901-2022, 2022.

Browne, E. C. and Cohen, R. C.: Effects of biogenic nitrate chemistry on the NO_x lifetime in remote continental regions, Atmospheric Chemistry and Physics, 12, 11917–11932, https://doi.org/10.5194/acp-12-11917-2012, 2012.

Burkholder, J. B., Sander, S. P., Abbatt, J., Barker, J. R., Cappa, C., Crounse, J. D., Dibble, T. S., Huie, R. E., Kolb, C. E., Kurylo, M. J., Orkin, V. L., Percival, C. J., Wilmouth, D. M., and Wine, P. H.: Chemical Kinetics and Photochemical Data for Use in Atmospheric Studies, Evaluation No. 19, Jet Propulsion Laboratory, Pasadena, CA, 2019.

Crippa, M., Guizzardi, D., Muntean, M., Schaaf, E., Dentener, F., van Aardenne, J. A., Monni, S., Doering, U., Olivier, J. G. J., Pagliari, V., and Janssens-Maenhout, G.: Gridded emissions of air pollutants for the period 1970–2012 within EDGAR v4.3.2, Earth System Science Data, 10, 1987–2013, https://doi.org/10.5194/essd-10-1987-2018, 2018.

Crounse, J. D., McKinney, K. A., Kwan, A. J., and Wennberg, P. O.: Measurement of Gas-Phase Hydroperoxides by Chemical Ionization Mass Spectrometry, Anal. Chem., 78, 6726–6732, https://doi.org/10.1021/ac0604235, 2006.

Crutzen, P. J. and Zimmermann, P. H.: The changing photochemistry of the troposphere, Tellus B, 43, 136–151, https://doi.org/10.1034/j.1600-0889.1991.t01-1-00012.x, 1991.

Dutta, I. and Heald, C. L.: Exploring Deposition Observations of Oxidized Sulfur and Nitrogen as a Constraint on Emissions in the United States, Journal of Geophysical Research: Atmospheres, 128, e2023JD039610, https://doi.org/10.1029/2023JD039610, 2023.

Dutta, I., Heald, C. L., Bourgeois, I., Crounse, J. D., Hintsa, E. J., Moore, F. L., and Peischl, J.: Characterizing the Global Tropospheric Budget of Oxidized Nitrogen (NOy), https://doi.org/10.5281/zenodo.18632688, 2026.

https://doi.org/10.5194/egusphere-2026-875
Preprint. Discussion started: 24 February 2026

Emerson, E. W., Hodshire, A. L., DeBolt, H. M., Bilsback, K. R., Pierce, J. R., McMeeking, G. R., and Farmer, D. K.: Revisiting particle dry deposition and its role in radiative effect estimates, Proceedings of the National Academy of Sciences, 117, 26076–26082, https://doi.org/10.1073/pnas.2014761117, 2020.

Fairlie, T. D., Jacob, D. J., and Park, R. J.: The impact of transpacific transport of mineral dust in the United States, Atmospheric Environment, 41, 1251–1266, https://doi.org/10.1016/j.atmosenv.2006.09.048, 2007.

Fischer, E. V., Jacob, D. J., Yantosca, R. M., Sulprizio, M. P., Millet, D. B., Mao, J., Paulot, F., Singh, H. B., Roiger, A., Ries, L., Talbot, R. W., Dzepina, K., and Pandey Deolal, S.: Atmospheric peroxyacetyl nitrate (PAN): a global budget and source attribution, Atmospheric Chemistry and Physics, 14, 2679–2698, https://doi.org/10.5194/acp-14-2679-2014, 2014.

Fisher, J. A., Jacob, D. J., Travis, K. R., Kim, P. S., Marais, E. A., Chan Miller, C., Yu, K., Zhu, L., Yantosca, R. M., Sulprizio, M. P., Mao, J., Wennberg, P. O., Crounse, J. D., Teng, A. P., Nguyen, T. B., St. Clair, J. M., Cohen, R. C., Romer, P., Nault, B. A., Wooldridge, P. J., Jimenez, J. L., Campuzano-Jost, P., Day, D. A., Hu, W., Shepson, P. B., Xiong, F., Blake, D. R., Goldstein, A. H., Misztal, P. K., Hanisco, T. F., Wolfe, G. M., Ryerson, T. B., Wisthaler, A., and Mikoviny, T.: Organic nitrate chemistry and its implications for nitrogen budgets in an isoprene- and monoterpene-rich atmosphere: constraints from aircraft (SEAC^{4}RS) and ground-based (SOAS) observations in the Southeast US, Atmospheric Chemistry and Physics, 16, 5969–5991, https://doi.org/10.5194/acp-16-5969-2016, 2016.

Fisher, J. A., Atlas, E. L., Barletta, B., Meinardi, S., Blake, D. R., Thompson, C. R., Ryerson, T. B., Peischl, J., Tzompa-Sosa, Z. A., and Murray, L. T.: Methyl, Ethyl, and Propyl Nitrates: Global Distribution and Impacts on Reactive Nitrogen in Remote Marine Environments, Journal of Geophysical Research: Atmospheres, 123, 12,429-12,451, https://doi.org/10.1029/2018JD029046, 2018.

Fountoukis, C. and Nenes, A.: ISORROPIA II: a computationally efficient thermodynamic equilibrium model for K^+–Ca^{2+}–Mg^{2+}–NH_4^+–Na^+–SO_4^{2-}–NO_3^-–Cl^-–H_2O aerosols, Atmospheric Chemistry and Physics, 7, 4639–4659, https://doi.org/10.5194/acp-7-4639-2007, 2007.

Guenther, A. B., Jiang, X., Heald, C. L., Sakulyanontvittaya, T., Duhl, T., Emmons, L. K., and Wang, X.: The Model of Emissions of Gases and Aerosols from Nature version 2.1 (MEGAN2.1): an extended and updated framework for modeling biogenic emissions, Geoscientific Model Development, 5, 1471–1492, https://doi.org/10.5194/gmd-5-1471-2012, 2012.

Hoesly, R. M., Smith, S. J., Feng, L., Klimont, Z., Janssens-Maenhout, G., Pitkanen, T., Seibert, J. J., Vu, L., Andres, R. J., Bolt, R. M., Bond, T. C., Dawidowski, L., Kholod, N., Kurokawa, J., Li, M., Liu, L., Lu, Z., Moura, M. C. P., O'Rourke, P. R., and Zhang, Q.: Historical (1750–2014) anthropogenic emissions of reactive gases and aerosols from the Community Emissions Data System (CEDS), Geoscientific Model Development, 11, 369–408, https://doi.org/10.5194/gmd-11-369-2018, 2018.

Holmes, C. D., Prather, M. J., and Vinken, G. C. M.: The climate impact of ship NO_x emissions: an improved estimate accounting for plume chemistry, Atmospheric Chemistry and Physics, 14, 6801–6812, https://doi.org/10.5194/acp-14-6801-2014, 2014.

Honrath, R. E., Peterson, M. C., Guo, S., Dibb, J. E., Shepson, P. B., and Campbell, B.: Evidence of NOx production within or upon ice particles in the Greenland snowpack, Geophysical Research Letters, 26, 695–698, https://doi.org/10.1029/1999GL900077, 1999.

Horowitz, L. W., Walters, S., Mauzerall, D. L., Emmons, L. K., Rasch, P. J., Granier, C., Tie, X., Lamarque, J.-F., Schultz, M. G., Tyndall, G. S., Orlando, J. J., and Brasseur, G. P.: A global simulation of tropospheric ozone and related tracers: Description and evaluation of MOZART, version 2, Journal of Geophysical Research: Atmospheres, 108, https://doi.org/10.1029/2002JD002853, 2003.

https://doi.org/10.5194/egusphere-2026-875
Preprint. Discussion started: 24 February 2026

Hu, L., Millet, D. B., Baasandorj, M., Griffis, T. J., Turner, P., Helmig, D., Curtis, A. J., and Hueber, J.: Isoprene emissions and impacts over an ecological transition region in the U.S. Upper Midwest inferred from tall tower measurements, Journal of Geophysical Research: Atmospheres, 120, 3553–3571, https://doi.org/10.1002/2014JD022732, 2015.

Hudman, R. C., Moore, N. E., Mebust, A. K., Martin, R. V., Russell, A. R., Valin, L. C., and Cohen, R. C.: Steps towards a mechanistic model of global soil nitric oxide emissions: implementation and space based-constraints, Atmospheric Chemistry and Physics, 12, 7779–7795, https://doi.org/10.5194/acp-12-7779-2012, 2012.

Huijnen, V., Williams, J., van Weele, M., van Noije, T., Krol, M., Dentener, F., Segers, A., Houweling, S., Peters, W., de Laat, J., Boersma, F., Bergamaschi, P., van Velthoven, P., Le Sager, P., Eskes, H., Alkemade, F., Scheele, R., Nédélec, P., and Pätz, H.-W.: The global chemistry transport model TM5: description and evaluation of the tropospheric chemistry version 3.0, Geoscientific Model Development, 3, 445–473, https://doi.org/10.5194/gmd-3-445-2010, 2010.

International GEOS-Chem User Community: GEOS-Chem v14.3.0, 2024.

Jacob, D. J.: Heterogeneous chemistry and tropospheric ozone, Atmospheric Environment, 34, 2131–2159, https://doi.org/10.1016/S1352-2310(99)00462-8, 2000.

Jacob, D. J., Logan, J. A., Yevich, R. M., Gardner, G. M., Spivakovsky, C. M., Wofsy, S. C., Munger, J. W., Sillman, S., Prather, M. J., Rodgers, M. O., Westberg, H., and Zimmerman, P. R.: Simulation of summertime ozone over North America, Journal of Geophysical Research: Atmospheres, 98, 14797–14816, https://doi.org/10.1029/93JD01223, 1993.

Kasibhatla, P., Sherwen, T., Evans, M. J., Carpenter, L. J., Reed, C., Alexander, B., Chen, Q., Sulprizio, M. P., Lee, J. D., Read, K. A., Bloss, W., Crilley, L. R., Keene, W. C., Pszenny, A. A. P., and Hodzic, A.: Global impact of nitrate photolysis in sea-salt aerosol on NO_x, OH, and O_3 in the marine boundary layer, Atmospheric Chemistry and Physics, 18, 11185–11203, https://doi.org/10.5194/acp-18-11185-2018, 2018.

Kasibhatla, P. S., Levy II, H., and Moxim, W. J.: Global NO , HNO3, PAN, and NO distributions from fossil fuel combustion emissions: A model study, Journal of Geophysical Research: Atmospheres, 98, 7165–7180, https://doi.org/10.1029/92JD02845, 1993.

Lamarque, J.-F., Dentener, F., McConnell, J., Ro, C.-U., Shaw, M., Vet, R., Bergmann, D., Cameron-Smith, P., Dalsoren, S., Doherty, R., Faluvegi, G., Ghan, S. J., Josse, B., Lee, Y. H., MacKenzie, I. A., Plummer, D., Shindell, D. T., Skeie, R. B., Stevenson, D. S., Strode, S., Zeng, G., Curran, M., Dahl-Jensen, D., Das, S., Fritzsche, D., and Nolan, M.: Multi-model mean nitrogen and sulfur deposition from the Atmospheric Chemistry and Climate Model Intercomparison Project (ACCMIP): evaluation of historical and projected future changes, Atmospheric Chemistry and Physics, 13, 7997–8018, https://doi.org/10.5194/acp-13-7997-2013, 2013.

Lavoie, G. A., Heywood, J. B., and Keck, J. C.: Experimental and Theoretical Study of Nitric Oxide Formation in Internal Combustion Engines, Combustion Science and Technology, 1, 313–326, https://doi.org/10.1080/00102206908952211, 1970.

Levy II, H.: Photochemistry of the lower troposphere, Planetary and Space Science, 20, 919–935, https://doi.org/10.1016/0032-0633(72)90177-8, 1972.

Levy II, H.: Photochemistry of minor constituents in the troposphere, Planetary and Space Science, 21, 575–591, https://doi.org/10.1016/0032-0633(73)90071-8, 1973.

Likens, G. E. and Bormann, F. H.: Acid Rain: A Serious Regional Environmental Problem, Science, 184, 1176–1179, https://doi.org/10.1126/science.184.4142.1176, 1974.

https://doi.org/10.5194/egusphere-2026-875
Preprint. Discussion started: 24 February 2026

Lin, H., Long, M. S., Sander, R., Sandu, A., Yantosca, R. M., Estrada, L. A., Shen, L., and Jacob, D. J.: An Adaptive Auto-Reduction Solver for Speeding Up Integration of Chemical Kinetics in Atmospheric Chemistry Models: Implementation and Evaluation in the Kinetic Pre-Processor (KPP) Version 3.0.0, Journal of Advances in Modeling Earth Systems, 15, e2022MS003293, https://doi.org/10.1029/2022MS003293, 2023.

Liu, H., Jacob, D. J., Bey, I., and Yantosca, R. M.: Constraints from 210Pb and 7Be on wet deposition and transport in a global three-dimensional chemical tracer model driven by assimilated meteorological fields, Journal of Geophysical Research: Atmospheres, 106, 12109–12128, https://doi.org/10.1029/2000JD900839, 2001.

Logan, J. A.: Nitrogen oxides in the troposphere: Global and regional budgets, Journal of Geophysical Research: Oceans, 88, 10785–10807, https://doi.org/10.1029/JC088iC15p10785, 1983.

Logan, J. A., Prather, M. J., Wofsy, S. C., and McElroy, M. B.: Tropospheric chemistry: A global perspective, Journal of Geophysical Research: Oceans, 86, 7210–7254, https://doi.org/10.1029/JC086iC08p07210, 1981.

Luo, G., Yu, F., and Schwab, J.: Revised treatment of wet scavenging processes dramatically improves GEOS-Chem 12.0.0 simulations of surface nitric acid, nitrate, and ammonium over the United States, Geoscientific Model Development, 12, 3439–3447, https://doi.org/10.5194/gmd-12-3439-2019, 2019.

Luo, G., Yu, F., and Moch, J. M.: Further improvement of wet process treatments in GEOS-Chem v12.6.0: impact on global distributions of aerosols and aerosol precursors, Geoscientific Model Development, 13, 2879–2903, https://doi.org/10.5194/gmd-13-2879-2020, 2020.

Martin, R. V., Jacob, D. J., Chance, K., Kurosu, T. P., Palmer, P. I., and Evans, M. J.: Global inventory of nitrogen oxide emissions constrained by space-based observations of NO2 columns, Journal of Geophysical Research: Atmospheres, 108, https://doi.org/10.1029/2003JD003453, 2003.

McDuffie, E. E., Smith, S. J., O'Rourke, P., Tibrewal, K., Venkataraman, C., Marais, E. A., Zheng, B., Crippa, M., Brauer, M., and Martin, R. V.: A global anthropogenic emission inventory of atmospheric pollutants from sector- and fuel-specific sources (1970–2017): an application of the Community Emissions Data System (CEDS), Earth System Science Data, 12, 3413–3442, https://doi.org/10.5194/essd-12-3413-2020, 2020.

Merryman, E. L. and Levy, A.: NOx Formation in CO Flames, United States Environmental Protection Agency, Research Triangle Park, NC, 1977.

Miyazaki, K., Eskes, H., Sudo, K., Boersma, K. F., Bowman, K., and Kanaya, Y.: Decadal changes in global surface NO_x emissions from multi-constituent satellite data assimilation, Atmospheric Chemistry and Physics, 17, 807–837, https://doi.org/10.5194/acp-17-807-2017, 2017.

Moore, F. L., Hintsa, E. J., Nance, D., Dutton, G., Hall, B., and Elkins, J. W.: ATom: Trace Gas Measurements from PANTHER Gas Chromatograph, https://doi.org/10.3334/ORNLDAAC/1914, 2022.

Moxim, W. J., Levy II, H., and Kasibhatla, P. S.: Simulated global tropospheric PAN: Its transport and impact on NO x, Journal of Geophysical Research: Atmospheres, 101, 12621–12638, https://doi.org/10.1029/96JD00338, 1996.

Murray, L. T., Jacob, D. J., Logan, J. A., Hudman, R. C., and Koshak, W. J.: Optimized regional and interannual variability of lightning in a global chemical transport model constrained by LIS/OTD satellite data, Journal of Geophysical Research: Atmospheres, 117, https://doi.org/10.1029/2012JD017934, 2012.

https://doi.org/10.5194/egusphere-2026-875
Preprint. Discussion started: 24 February 2026

Murray, L. T., Fiore, A. M., Shindell, D. T., Naik, V., and Horowitz, L. W.: Large uncertainties in global hydroxyl projections tied to fate of reactive nitrogen and carbon, Proceedings of the National Academy of Sciences, 118, e2115204118, https://doi.org/10.1073/pnas.2115204118, 2021.

Norman, O. G., Heald, C. L., Campuzano-Jost, P., Coe, H., Fiddler, M. N., Green, J. R., Jimenez, J. L., Kaiser, K., Liao, J., Middlebrook, A. M., Nault, B. A., Nowak, J. B., Schneider, J., and Welti, A.: Exploring the processes controlling secondary inorganic aerosol: Evaluating the global GEOS-Chem simulation using a suite of aircraft campaigns, EGUsphere, 1–37, https://doi.org/10.5194/egusphere-2024-2296, 2024.

Paerl, H. W. and Whitall, D. R.: Anthropogenically-Derived Atmospheric Nitrogen Deposition, Marine Eutrophication and Harmful Algal Bloom Expansion: Is There a Link?, Ambio, 28, 307–311, 1999.

Park, R. J., Jacob, D. J., Field, B. D., Yantosca, R. M., and Chin, M.: Natural and transboundary pollution influences on sulfate-nitrate-ammonium aerosols in the United States: Implications for policy, Journal of Geophysical Research: Atmospheres, 109, https://doi.org/10.1029/2003JD004473, 2004.

Perner, D. and Platt, U.: Detection of nitrous acid in the atmosphere by differential optical absorption, Geophysical Research Letters, 6, 917–920, https://doi.org/10.1029/GL006i012p00917, 1979.

Philip, S., Martin, R. V., and Keller, C. A.: Sensitivity of chemistry-transport model simulations to the duration of chemical and transport operators: a case study with GEOS-Chem v10-01, Geoscientific Model Development, 9, 1683–1695, https://doi.org/10.5194/gmd-9-1683-2016, 2016.

Pitts Jr., J. N., Sanhueza, E., Atkinson, R., Carter, W. P. L., Winer, A. M., Harris, G. W., and Plum, C. N.: An investigation of the dark formation of nitrous acid in environmental chambers, International Journal of Chemical Kinetics, 16, 919–939, https://doi.org/10.1002/kin.550160712, 1984.

Pye, H. O. T., Liao, H., Wu, S., Mickley, L. J., Jacob, D. J., Henze, D. K., and Seinfeld, J. H.: Effect of changes in climate and emissions on future sulfate-nitrate-ammonium aerosol levels in the United States, Journal of Geophysical Research: Atmospheres, 114, https://doi.org/10.1029/2008JD010701, 2009.

Rastigejev, Y., Park, R., Brenner, M. P., and Jacob, D. J.: Resolving intercontinental pollution plumes in global models of atmospheric transport, Journal of Geophysical Research: Atmospheres, 115, https://doi.org/10.1029/2009JD012568, 2010.

Reed, C., Evans, M. J., Crilley, L. R., Bloss, W. J., Sherwen, T., Read, K. A., Lee, J. D., and Carpenter, L. J.: Evidence for renoxification in the tropical marine boundary layer, Atmospheric Chemistry and Physics, 17, 4081–4092, https://doi.org/10.5194/acp-17-4081-2017, 2017.

Ridley, D. A., Heald, C. L., and Ford, B.: North African dust export and deposition: A satellite and model perspective, Journal of Geophysical Research: Atmospheres, 117, https://doi.org/10.1029/2011JD016794, 2012.

Romer, P. S., Wooldridge, P. J., Crounse, J. D., Kim, M. J., Wennberg, P. O., Dibb, J. E., Scheuer, E., Blake, D. R., Meinardi, S., Brosius, A. L., Thames, A. B., Miller, D. O., Brune, W. H., Hall, S. R., Ryerson, T. B., and Cohen, R. C.: Constraints on Aerosol Nitrate Photolysis as a Potential Source of HONO and NOx, Environ. Sci. Technol., 52, 13738–13746, https://doi.org/10.1021/acs.est.8b03861, 2018.

Romer Present, P. S., Zare, A., and Cohen, R. C.: The changing role of organic nitrates in the removal and transport of NO_x, Atmospheric Chemistry and Physics, 20, 267–279, https://doi.org/10.5194/acp-20-267-2020, 2020.

https://doi.org/10.5194/egusphere-2026-875
Preprint. Discussion started: 24 February 2026

Rowlinson, M. J., Carpenter, L. J., Evans, M. J., Lee, J. D., Andersen, S. T., Sherwen, T., Callaghan, A. B., Sommariva, R., Bloss, W., Hou, S., Crilley, L. R., Pfeilsticker, K., Weyland, B., Ryerson, T. B., Veres, P. R., Campuzano-Jost, P., Guo, H., Nault, B. A., Jimenez, J. L., and Fomba, K. W.: A nitrate photolysis source of tropospheric HONO is incompatible with current understanding of atmospheric chemistry, Atmospheric Chemistry and Physics, 25, 16945–16968, https://doi.org/10.5194/acp-25-16945-2025, 2025.

Ryerson, T. B., Williams, E. J., and Fehsenfeld, F. C.: An efficient photolysis system for fast-response NO2 measurements, Journal of Geophysical Research: Atmospheres, 105, 26447–26461, https://doi.org/10.1029/2000JD900389, 2000.

Ryerson, T. B., Thompson, C. R., Peischl, J., and Bourgeois, I.: ATom: L2 In Situ Measurements from NOAA Nitrogen Oxides and Ozone (NOyO3) Instrument, https://doi.org/10.3334/ORNLDAAC/1734, 2019.

Sander, R., Baumgaertner, A., Cabrera-Perez, D., Frank, F., Gromov, S., Grooß, J.-U., Harder, H., Huijnen, V., Jöckel, P., Karydis, V. A., Niemeyer, K. E., Pozzer, A., Riede, H., Schultz, M. G., Taraborrelli, D., and Tauer, S.: The community atmospheric chemistry box model CAABA/MECCA-4.0, Geoscientific Model Development, 12, 1365–1385, https://doi.org/10.5194/gmd-12-1365-2019, 2019.

Sandu, A., Sander, R., Long, M. S., Yantosca, R. M., Lin, H., Shen, L., and Jacob, D. J.: KineticPreProcessor/KPP: The Kinetic PreProcessor (KPP) 3.0.2, , https://doi.org/10.5281/zenodo.8030063, 2023.

Schindler, D. W.: Eutrophication and Recovery in Experimental Lakes: Implications for Lake Management, Science, 184, 897–899, 1974.

Seinfeld, J. H. and Pandis, S. N.: Atmospheric chemistry and physics: from air pollution to climate change, John Wiley & Sons, 2016.

Shah, V., Jacob, D. J., Dang, R., Lamsal, L. N., Strode, S. A., Steenrod, S. D., Boersma, K. F., Eastham, S. D., Fritz, T. M., Thompson, C., Peischl, J., Bourgeois, I., Pollack, I. B., Nault, B. A., Cohen, R. C., Campuzano-Jost, P., Jimenez, J. L., Andersen, S. T., Carpenter, L. J., Sherwen, T., and Evans, M. J.: Nitrogen oxides in the free troposphere: implications for tropospheric oxidants and the interpretation of satellite NO_2 measurements, Atmospheric Chemistry and Physics, 23, 1227–1257, https://doi.org/10.5194/acp-23-1227-2023, 2023.

Shi, Q., Tao, Y., Krechmer, J. E., Heald, C. L., Murphy, J. G., Kroll, J. H., and Ye, Q.: Laboratory Investigation of Renoxification from the Photolysis of Inorganic Particulate Nitrate, Environ. Sci. Technol., 55, 854–861, https://doi.org/10.1021/acs.est.0c06049, 2021.

Silvern, R. F., Jacob, D. J., Travis, K. R., Sherwen, T., Evans, M. J., Cohen, R. C., Laughner, J. L., Hall, S. R., Ullmann, K., Crounse, J. D., Wennberg, P. O., Peischl, J., and Pollack, I. B.: Observed NO/NO2 Ratios in the Upper Troposphere Imply Errors in NO-NO2-O3 Cycling Kinetics or an Unaccounted NOx Reservoir, Geophysical Research Letters, 45, 4466–4474, https://doi.org/10.1029/2018GL077728, 2018.

Singh, H. B. and Hanst, P. L.: Peroxyacetyl nitrate (PAN) in the unpolluted atmosphere: An important reservoir for nitrogen oxides, Geophysical Research Letters, 8, 941–944, https://doi.org/10.1029/GL008i008p00941, 1981.

Singh, H. B., Salas, L., Herlth, D., Kolyer, R., Czech, E., Avery, M., Crawford, J. H., Pierce, R. B., Sachse, G. W., Blake, D. R., Cohen, R. C., Bertram, T. H., Perring, A., Wooldridge, P. J., Dibb, J., Huey, G., Hudman, R. C., Turquety, S., Emmons, L. K., Flocke, F., Tang, Y., Carmichael, G. R., and Horowitz, L. W.: Reactive nitrogen distribution and partitioning in the North American troposphere and lowermost stratosphere, Journal of Geophysical Research: Atmospheres, 112, https://doi.org/10.1029/2006JD007664, 2007.

https://doi.org/10.5194/egusphere-2026-875
Preprint. Discussion started: 24 February 2026

Staudt, A. C., Jacob, D. J., Ravetta, F., Logan, J. A., Bachiochi, D., Krishnamurti, T. N., Sandholm, S., Ridley, B., Singh, H. B., and Talbot, B.: Sources and chemistry of nitrogen oxides over the tropical Pacific, Journal of Geophysical Research: Atmospheres, 108, https://doi.org/10.1029/2002JD002139, 2003.

Thompson, C. R., Wofsy, S. C., Prather, M. J., Newman, P. A., Hanisco, T. F., Ryerson, T. B., Fahey, D. W., Apel, E. C., Brock, C. A., Brune, W. H., Froyd, K., Katich, J. M., Nicely, J. M., Peischl, J., Ray, E., Veres, P. R., Wang, S., Allen, H. M., Asher, E., Bian, H., Blake, D., Bourgeois, I., Budney, J., Bui, T. P., Butler, A., Campuzano-Jost, P., Chang, C., Chin, M., Commane, R., Correa, G., Crounse, J. D., Daube, B., Dibb, J. E., DiGangi, J. P., Diskin, G. S., Dollner, M., Elkins, J. W., Fiore, A. M., Flynn, C. M., Guo, H., Hall, S. R., Hannun, R. A., Hills, A., Hintsa, E. J., Hodzic, A., Hornbrook, R. S., Huey, L. G., Jimenez, J. L., Keeling, R. F., Kim, M. J., Kupc, A., Lacey, F., Lait, L. R., Lamarque, J.-F., Liu, J., McKain, K., Meinardi, S., Miller, D. O., Montzka, S. A., Moore, F. L., Morgan, E. J., Murphy, D. M., Murray, L. T., Nault, B. A., Neuman, J. A., Nguyen, L., Gonzalez, Y., Rollins, A., Rosenlof, K., Sargent, M., Schill, G., Schwarz, J. P., Clair, J. M. S., Steenrod, S. D., Stephens, B. B., Strahan, S. E., Strode, S. A., Sweeney, C., Thames, A. B., Ullmann, K., Wagner, N., Weber, R., Weinzierl, B., Wennberg, P. O., Williamson, C. J., Wolfe, G. M., and Zeng, L.: The NASA Atmospheric Tomography (ATom) Mission: Imaging the Chemistry of the Global Atmosphere, Bulletin of the American Meteorological Society, 103, E761–E790, https://doi.org/10.1175/BAMS-D-20-0315.1, 2022.

Travis, K. R., Jacob, D. J., Fisher, J. A., Kim, P. S., Marais, E. A., Zhu, L., Yu, K., Miller, C. C., Yantosca, R. M., Sulprizio, M. P., Thompson, A. M., Wennberg, P. O., Crounse, J. D., St. Clair, J. M., Cohen, R. C., Laughner, J. L., Dibb, J. E., Hall, S. R., Ullmann, K., Wolfe, G. M., Pollack, I. B., Peischl, J., Neuman, J. A., and Zhou, X.: Why do models overestimate surface ozone in the Southeast United States?, Atmospheric Chemistry and Physics, 16, 13561–13577, https://doi.org/10.5194/acp-16-13561-2016, 2016.

Travis, K. R., Heald, C. L., Allen, H. M., Apel, E. C., Arnold, S. R., Blake, D. R., Brune, W. H., Chen, X., Commane, R., Crounse, J. D., Daube, B. C., Diskin, G. S., Elkins, J. W., Evans, M. J., Hall, S. R., Hintsa, E. J., Hornbrook, R. S., Kasibhatla, P. S., Kim, M. J., Luo, G., McKain, K., Millet, D. B., Moore, F. L., Peischl, J., Ryerson, T. B., Sherwen, T., Thames, A. B., Ullmann, K., Wang, X., Wennberg, P. O., Wolfe, G. M., and Yu, F.: Constraining remote oxidation capacity with ATom observations, Atmospheric Chemistry and Physics, 20, 7753–7781, https://doi.org/10.5194/acp-20-7753-2020, 2020.

US EPA: Our Nation's Air: Trends Through 2023, United States Environmental Protection Agency, 2024.

Wang, X., Jacob, D. J., Downs, W., Zhai, S., Zhu, L., Shah, V., Holmes, C. D., Sherwen, T., Alexander, B., Evans, M. J., Eastham, S. D., Neuman, J. A., Veres, P. R., Koenig, T. K., Volkamer, R., Huey, L. G., Bannan, T. J., Percival, C. J., Lee, B. H., and Thornton, J. A.: Global tropospheric halogen (Cl, Br, I) chemistry and its impact on oxidants, Atmospheric Chemistry and Physics, 21, 13973–13996, https://doi.org/10.5194/acp-21-13973-2021, 2021.

Wang, Y., Jacob, D. J., and Logan, J. A.: Global simulation of tropospheric O3-NOx-hydrocarbon chemistry: 1. Model formulation, Journal of Geophysical Research: Atmospheres, 103, 10713–10725, https://doi.org/10.1029/98JD00158, 1998a.

Wang, Y., Logan, J. A., and Jacob, D. J.: Global simulation of tropospheric O3-NOx-hydrocarbon chemistry: 2. Model evaluation and global ozone budget, Journal of Geophysical Research: Atmospheres, 103, 10727–10755, https://doi.org/10.1029/98JD00157, 1998b.

Weng, H., Lin, J., Martin, R., Millet, D. B., Jaeglé, L., Ridley, D., Keller, C., Li, C., Du, M., and Meng, J.: Global high-resolution emissions of soil NOx, sea salt aerosols, and biogenic volatile organic compounds, Sci Data, 7, 148, https://doi.org/10.1038/s41597-020-0488-5, 2020.

Wesely, M. L.: Parameterization of surface resistances to gaseous dry deposition in regional-scale numerical models, Atmospheric Environment (1967), 23, 1293–1304, https://doi.org/10.1016/0004-6981(89)90153-4, 1989.

https://doi.org/10.5194/egusphere-2026-875
Preprint. Discussion started: 24 February 2026

Wofsy, S. C., Afshar, S., Allen, H. M., Apel, E. C., Asher, E. C., Barletta, B., Bent, J., Bian, H., Biggs, B. C., Blake, D. R., Blake, N., Bourgeois, I., Brock, C. A., Brune, W. H., Budney, J. W., Bui, T. P., Butler, A., Campuzano-Jost, P., Chang, C. S., Chin, M., Commane, R., Correa, G., Crounse, J. D., Cullis, P. D., Daube, B. C., Day, D. A., Dean-Day, J. M., Dibb, J. E., Digangi, J. P., Diskin, G. S., Dollner, M., Elkins, J. W., Erdesz, F., Fiore, A. M., Flynn, C. M., Froyd, K. D., Gesler, D. W., Hall, S. R., Hanisco, T. F., Hannun, R. A., Hills, A. J., Hintsa, E. J., Hoffman, A., Hornbrook, R. S., Huey, L. G., Hughes, S., Jimenez, J. L., Johnson, B. J., Katich, J. M., Keeling, R. F., Kim, M. J., Kupc, A., Lait, L. R., Lamarque, J.-F., Liu, J., Mckain, K., Mclaughlin, R. J., Meinardi, S., Miller, D. O., Montzka, S. A., Moore, F. L., Morgan, E. J., Murphy, D. M., Murray, L. T., Nault, B. A., Neuman, J. A., Newman, P. A., Nicely, J. M., Pan, X., Paplawsky, W., Peischl, J., Prather, M. J., Price, D. J., Ray, E. A., Reeves, J. M., Richardson, M., Rollins, A. W., Rosenlof, K. H., Ryerson, T. B., Scheuer, E., Schill, G. P., Schroder, J. C., Schwarz, J. P., St. Clair, J. M., Steenrod, S. D., Stephens, B. B., Strode, S. A., Sweeney, C., Tanner, D., Teng, A. P., Thames, A. B., Thompson, C. R., Ullmann, K., Veres, P. R., Vizenor, N., Wagner, N. L., Watt, A., Weber, R., Weinzierl, B. B., et al.: ATom: Merged Atmospheric Chemistry, Trace Gases, and Aerosols, https://doi.org/10.3334/ORNLDAAC/1581, 2018.

Wofsy, S. C., Afshar, S., Allen, H. M., Apel, E. C., Asher, E. C., Barletta, B., Bent, J., Bian, H., Biggs, B. C., Blake, D. R., Blake, N., Bourgeois, I., Brock, C. A., Brune, W. H., Budney, J. W., Bui, T. P., Butler, A., Campuzano-Jost, P., Chang, C. S., Chin, M., Commane, R., Correa, G., Crounse, J. D., Cullis, P. D., Daube, B. C., Day, D. A., Dean-Day, J. M., Dibb, J. E., Digangi, J. P., Diskin, G. S., Dollner, M., Elkins, J. W., Erdesz, F., Fiore, A. M., Flynn, C. M., Froyd, K. D., Gesler, D. W., Hall, S. R., Hanisco, T. F., Hannun, R. A., Hills, A. J., Hintsa, E. J., Hoffman, A., Hornbrook, R. S., Huey, L. G., Hughes, S., Jimenez, J. L., Johnson, B. J., Katich, J. M., Keeling, R. F., Kim, M. J., Kupc, A., Lait, L. R., Mckain, K., Mclaughlin, R. J., Meinardi, S., Miller, D. O., Montzka, S. A., Moore, F. L., Morgan, E. J., Murphy, D. M., Murray, L. T., Nault, B. A., Neuman, J. A., Newman, P. A., Nicely, J. M., Pan, X., Paplawsky, W., Peischl, J., Prather, M. J., Price, D. J., Ray, E. A., Reeves, J. M., Richardson, M., Rollins, A. W., Rosenlof, K. H., Ryerson, T. B., Scheuer, E., Schill, G. P., Schroder, J. C., Schwarz, J. P., St. Clair, J. M., Steenrod, S. D., Stephens, B. B., Strode, S. A., Sweeney, C., Tanner, D., Teng, A. P., Thames, A. B., Thompson, C. R., Ullmann, K., Veres, P. R., Wagner, N. L., Watt, A., Weber, R., Weinzierl, B. B., Wennberg, P. O., Williamson, C. J., Wilson, J. C., et al.: ATom: Merged Atmospheric Chemistry, Trace Gases, and Aerosols, Version 2, https://doi.org/10.3334/ORNLDAAC/1925, 2021.

Ye, C., Gao, H., Zhang, N., and Zhou, X.: Photolysis of Nitric Acid and Nitrate on Natural and Artificial Surfaces, Environ. Sci. Technol., 50, 3530–3536, https://doi.org/10.1021/acs.est.5b05032, 2016a.

Ye, C., Zhou, X., Pu, D., Stutz, J., Festa, J., Spolaor, M., Tsai, C., Cantrell, C., Mauldin, R. L., Campos, T., Weinheimer, A., Hornbrook, R. S., Apel, E. C., Guenther, A., Kaser, L., Yuan, B., Karl, T., Haggerty, J., Hall, S., Ullmann, K., Smith, J. N., Ortega, J., and Knote, C.: Rapid cycling of reactive nitrogen in the marine boundary layer, Nature, 532, 489–491, https://doi.org/10.1038/nature17195, 2016b.

Ye, C., Zhang, N., Gao, H., and Zhou, X.: Photolysis of Particulate Nitrate as a Source of HONO and NOx, Environ. Sci. Technol., 51, 6849–6856, https://doi.org/10.1021/acs.est.7b00387, 2017.

Zare, A., Romer, P. S., Nguyen, T., Keutsch, F. N., Skog, K., and Cohen, R. C.: A comprehensive organic nitrate chemistry: insights into the lifetime of atmospheric organic nitrates, Atmospheric Chemistry and Physics, 18, 15419–15436, https://doi.org/10.5194/acp-18-15419-2018, 2018.

Zel'dovich, Y. B.: The Oxidation of Nitrogen in Combustion and Explosions, Acta Physicochimica, 21, 577–628, 1946.

Zhang, L., Gong, S., Padro, J., and Barrie, L.: A size-segregated particle dry deposition scheme for an atmospheric aerosol module, Atmospheric Environment, 35, 549–560, https://doi.org/10.1016/S1352-2310(00)00326-5, 2001.

https://doi.org/10.5194/egusphere-2026-875
Preprint. Discussion started: 24 February 2026

Zhang, L., Jacob, D. J., Knipping, E. M., Kumar, N., Munger, J. W., Carouge, C. C., van Donkelaar, A., Wang, Y. X., and Chen, D.: Nitrogen deposition to the United States: distribution, sources, and processes, Atmospheric Chemistry and
790 Physics, 12, 4539–4554, https://doi.org/10.5194/acp-12-4539-2012, 2012.